Molecular Biology of the Cell
Vol. 15, 4321–4336, September 2004

Transcriptional Response of Yeast to Aflatoxin B_1: Recombinational Repair Involving *RAD51* and *RAD1*

Monika U. Keller-Seitz,* Ulrich Certa,† Christian Sengstag,* Friedrich E. Würgler,* Mingzeng Sun,‡ and Michael Fasullo‡§

*Institute of Toxicology, Swiss Federal Institute of Technology ETH, CH-8603 Schwerzenbach, Switzerland; †Pharma Division, F. Hoffmann-La Roche Ltd., CH-4070 Basel, Switzerland; and ‡Ordway Research Institute, Albany, NY 12208-03479

Submitted May 7, 2004; Revised June 9, 2004; Accepted June 14, 2004
Monitoring Editor: Keith Yamamoto

The potent carcinogen aflatoxin B_1 is a weak mutagen but a strong recombinagen in *Saccharomyces cerevisiae*. Aflatoxin B_1 exposure greatly increases frequencies of both heteroallelic recombination and chromosomal translocations. We analyzed the gene expression pattern of diploid cells exposed to aflatoxin B_1 using high-density oligonucleotide arrays comprising specific probes for all 6218 open reading frames. Among 183 responsive genes, 46 are involved in either DNA repair or in control of cell growth and division. Inducible growth control genes include those in the TOR signaling pathway and *SPO12*, whereas *PKC1* is downregulated. Eleven of the 15 inducible DNA repair genes, including *RAD51*, participate in recombination. Survival and translocation frequencies are reduced in the *rad51* diploid after aflatoxin B_1 exposure. In *mec1* checkpoint mutants, aflatoxin B_1 exposure does not induce *RAD51* expression or increase translocation frequencies; however, when *RAD51* is constitutively overexpressed in the *mec1* mutant, aflatoxin B_1 exposure increased translocation frequencies. Thus the transcriptional profile after aflatoxin B_1 exposure may elucidate the genotoxic properties of aflatoxin B_1.

INTRODUCTION

The fungal mycotoxin aflatoxin B_1 (AFB_1) is a potent carcinogen, and low levels of chronic exposure correlate with increased neoplasia, primarily liver cancer, in humans (Hsu *et al.*, 1991; Shen and Ong, 1996; Wogan, 1999) and in many animal species (Eaton and Gallagher, 1994). At the low doses observed in chronic human exposure, the carcinogenic potential of AFB_1 is correlated with DNA adduct formation (Bailey, 1994; Buss *et al.*, 1990; Otteneder and Lutz, 1999). As demonstrated by epidemiological studies, a G-to-T transversion in the codon 249 of the *p53* gene is often found in AFB_1-associated hepatocellular carcinoma (Eaton and Gallagher, 1994). Although mutation in the *p53* tumor suppressor gene may be an important etiologic factor in AFB_1-induced liver cancer in humans, animal studies suggest that loss of *p53* function is not a strict requirement. Other effects of AFB_1 or other enhancers of cell proliferation, such as hepatitis B virus infection, are likely required (Eaton and Gallagher, 1994). Further elucidation of the genotoxic effects of AFB_1 may thus improve our understanding of its potent carcinogenicity.

AFB_1 is a mutagen in *Saccharomyces cerevisiae* (Sengstag *et al.*, 1996), *Escherichia coli*, rainbow trout, mice, rat and human cells (reviewed in Smela *et al.*, 2001), and a recombinagen in yeast and in human cells (Stettler and Sengstag, 2001). In yeast, AFB_1 can induce mitotic, homologous recombination resulting in heteroallelic gene conversion and translocations (Sengstag *et al.*, 1996). After yeast cells are exposed to low doses of AFB_1 in the expected range of human exposure, there is a strong stimulation of recombination but not mutation (unpublished data). In human lymphoblastoid cell line TK6, AFB_1 exposure increases heteroallelic recombination at the thymidine kinase locus resulting in loss of heterozygosity (Stettler and Sengstag, 2001). Thus, understanding the molecular basis for the recombinogenicity of AFB_1 in yeast may help understand the potent carcinogenicity of AFB_1 compared with toxins with similar mutagenicity.

The remarkable recombinogenicity of AFB_1 may result from a combination of factors. First, specific AFB_1-DNA adducts may enzymatically or spontaneously convert to DNA double-strand breaks, thus directly initiating recombination. The N^7 adduct 8,9-dihydro-8-(N^7-guanyl)-9-hydroxyaflatoxin B_1 is the major product in vitro (Essigmann *et al.*, 1977) and in vivo (Lin *et al.*, 1977; Croy *et al.*, 1978). The positively charged imidazole ring of the principal DNA adduct promotes depurination, giving rise to an apurinic (AP) site, which can further yield single-strand breaks by β-elimination (Friedberg *et al.*, 1995). Clusters of these single-strand breaks could yield double-strand breaks. Alternatively, mildly alkaline conditions can subsequently result in the formation of a chemically and biologically stable foramidopyrimidine derivative (AFB_1-FAPY), which represents a significant product in vivo (Croy and Wogan, 1981). AP sites can be removed by the base excision repair (BER) pathway, and the AFB_1-N^7-guanine adducts can be removed by the nucleotide excision repair (NER; Leadon *et al.*, 1981). The AFB_1-FAPY adduct, however, is a nonrepairable, persistent lesion (Martin and Garner, 1977) that interferes with DNA replication. Such interference could indirectly stimulate recombination (Friedberg *et al.*, 1995) and generate DNA

Article published online ahead of print. Mol. Biol. Cell 10.1091/mbc.E04–05–0375. Article and publication date are available at www.molbiolcell.org/cgi/doi/10.1091/mbc.E04–05–0375.

§ Corresponding author. E-mail address: mfasullo@ordwayresearch.org.

double-strand breaks. However, chromosomal fragments have not been detected by pulse-field electrophoresis after yeast cells were exposed to AFB_1 (unpublished data).

Alternatively, exposure to AFB_1 could also elicit a stress response in yeast that stimulates more recombination than mutation. We thus investigated the global cellular response to a 4-h. exposure to AFB_1. DNA microarrays have been used successfully in yeast to investigate the global transcriptional response after exposure to saline (Posas *et al.*, 2000), methyl methanesulfonate (MMS; Jelinsky and Samson, 1999, Gasch *et al.*, 2000), and ionizing radiation (Gasch *et al.*, 2001). The current mRNA expression analysis shows that a large fraction of the AFB_1-induced genes is involved in maintenance of DNA integrity. Because the majority of the transcriptionally upregulated DNA repair genes belong to the NER or recombinational repair (RR) pathway, we exposed the respective *rad1* and *rad51* repair mutants to AFB_1 and measured translocation frequencies. To strengthen the correlation between AFB_1-associated recombination and *RAD51* induction, we measured AFB_1-associated recombination in *mec1* checkpoint mutants, defective in the DNA damage inducibility of *RAD51,* and in *mec1* mutants expressing higher basal levels of *RAD51*. Our data suggest that AFB_1 upregulates a recombinational repair pathway that involves *RAD51* and *RAD1*.

MATERIALS AND METHODS

Media and Strains

Standard media, including YM medium (0.76% yeast nitrogen base without amino acids, 2% glucose), YM medium supplemented with appropriate amino acids, and YPD medium (yeast extract, peptone, dextrose) were used for the culture of yeast strains. Amino acids, adenine, and uracil were purchased from Merck (Dietikon, Switzerland), yeast nitrogen base, and bacto agar from Difco (Chemie Brunschwig, Basel, Switzerland).

Yeast strains contain two overlapping *his3* fragments on chromosomes II and IV and were derived from YB109 (Fasullo and Dave, 1994). Translocation frequencies were determined by selecting for His^+ recombinants that are generated by mitotic recombination between the *his3* fragments. (Fasullo and Davis, 1987). YMK2181 (*MAT**a**/MATα, ura3-52/ura3-52, his3-Δ200/his3-Δ200, ade2-101/ade2-101, trp1-Δ1/TRP1, gal3-/gal3-, leu2-3112/leu2-3112, GAL1::his3-Δ5′/GAL1::his3-Δ5′, trp1::his3-Δ3′/trp1::his3-Δ3′, leu2-Δ3′, leu2-Δ5′, kanMX4, HOcs*), and YB110 (*MAT**a**/MATα, ade2-101/ade2-101, ura3-52/ura3-52, his3-Δ200/his3-Δ200, trp1-Δ1/trp1-Δ1, leu2/LEU2, GAL1::his3-Δ5′/GAL1, trp1::his3Δ3′/trp1-Δ1, LYS2/lys2-801*; Fasullo and Dave, 1994) have been previously used to measure DNA damage-associated translocation. YB150 (*rad1*) and YB195 (*rad51*) are identical to YB110 (Rad^+) except for the *rad51* and *rad1* disruptions, respectively. We replaced the *ade2-101* allele in YB109 and with *ade2-n* (YB318) and the *ade2-101* allele in YA102 with *ade2-a* (YB336) by two-step gene replacement using the plasmid pKH9 (Huang and Symington, 1994).

mec1 checkpoint mutants that measure AFB_1-associated translocations contain either *mec1-21* or the *mec1* null mutation. The original *MATα mec1-21* (YA16) strain is derived from W303 (Sanchez *et al.*, 1996). We backcrossed YA16 10 times with strains in the S288c background (YB163 and FY251 [Dong and Fasullo, 2003] and YB336) to generate meiotic segregants YB316 (*MATα ura3-52 his3-Δ200, trp1-Δ1, ade2-a, mec1-21*) and YB314 (*MATα ura3-52 his3-Δ200, trp1Δ-1, ADE2, mec1-21*) by tetrad dissections. YB318 was crossed with YB314 to generate the meiotic segregant YB319 (*MAT**a**-inc, ura3-52, his3-Δ200, ade2-n, trp1-Δ1, leu2, lys2, GAL1::his3-Δ5′, trp1::his3-Δ3′, mec1-21*). YB325 (*MAT**a**/MATα, ade2-a/ade2-n, ura3-52/ura3-52, his3-Δ200/his3-Δ200, trp1-Δ1/trp1-Δ1, leu2/LEU2, GAL1::his3-Δ5′/GAL1, trp1::his3-Δ3′/trp1-Δ1, lys3–801/lys2-801, mec1-21/mec1-21*) was then used to measure translocations and heteroallelic recombination in the *mec1-21* background. To measure translocations in the *mec1* null mutant, we first introduced the *sml1::kanMX* allele in YB318 and YB315 by PCR-mediated gene replacement (Goldstein and McCusker, 1999) to make YB320 and YB317, respectively, because lethality conferred by *mec1* deletions is suppressed by *sml1* mutations (Zhao *et al.*, 1998). YB323 (*MAT**a**/MATα, ade2-a/ade2-n, ura3-52/ura3-52, his3-Δ200/his3-Δ200, trp1-Δ1/trp1-Δ1, leu2/LEU2, GAL1::his3-Δ5′/GAL1, sml1::kanMX/sml1::kanMX, trp1::his3Δ3′/trp1-Δ1, lys2–801/lys2–801*) was then derived by a diploid cross of YB320 and YB317. The *mec1Δ::TRP1* allele (Zhao *et al.*, 2000) was introduced into YB320 and YB317 to make YB321 and YB322, respectively. YB324 (*MAT**a**/MATα, ade2-a/ade2-n, ura3-52/ura3-52, his3-Δ200/his3-Δ200, trp1-Δ1/trp1-Δ1, leu2/LEU2, GAL1::his3-Δ5′/GAL1, sml1::kanMX/sml1::kanMX, trp1::his3Δ3′/trp1-Δ1, lys2–801/lys2–801, mec1Δ::TRP1/mec1Δ::TRP1*) was then derived by a diploid cross. To overexpress *RAD51* in the *mec1* mutants, pR51.3 (Leu^+), containing *RAD51* on a 2 μ plasmid, was introduced into YB325 (Sung and Stratton, 1996).

The 2 μ *URA3* plasmids pMK637 (this work) or pSB229 (Eugster *et al.*, 1992), containing *hCYP1A2+hOR* and *hCYP1A1+hOR* cDNAs, respectively, or the *LEU2* plasmid pCS512 (Sengstag *et al.*, 1996), containing *hCYP1A1+hOR* cDNAs, were first introduced into yeast strains by DNA transformation to metabolically activate the AFB_1 and benzo-(*a*)-pyrene-7,8-dihydrodiol (BaP-DHD; Klebe *et al.*, 1983). The 2 μ *URA3* plasmid pCS316, containing the *hCYP1A1+hOR* cDNA in the opposite orientation as in pSB229 (Eugster *et al.*, 1992), was introduced into YB110, YB324, and YB335 to measure AFB_1-associated translocations in *mec1* checkpoint mutants. pMK637 was introduced into the strain YMK2181 to measure AFB_1 related-changes in gene expression using the oligonucleotide arrays. pCS512 was introduced into YB150 and the plasmid pSB229 was introduced into YB195 and YB110 to measure chromosomal translocation frequency and drug killing after exposure to ethyl methanesulfonate (EMS), AFB_1, and BaP-DHD.

Exposure of Yeast Strains to DNA-damaging Agents

In brief, exponentially growing yeast cells were collected by centrifugation and resuspended in 0.1 M sodium phosphate buffer (pH 7.5); the final cell density was 4×10^8 cells/ml. To measure the stimulation of recombination, 1 ml of the cells in 0.1 M sodium phosphate buffer (pH 7.5) was exposed to chemicals for 4 h. at 30°C in a rotary shaker. The cells were then pelleted in a clinical centrifuge, washed, and diluted in supplemented minimal medium. To measure the net frequencies of recombination, the spontaneous frequencies were subtracted from the DNA damage–associated frequency. To measure AFB_1-associated changes in gene expression, 2 ml of cells in 0.1 M sodium phosphate buffer was exposed to 25 μM AFB_1 for 4 h at 30°C in a rotary shaker. Cells were then centrifuged and resuspended in the appropriate buffers to extract nucleic acids.

Preparation of Nucleic Acids for Oligonucleotide Arrays and Hybridization

After AFB_1 exposure, cells were washed once, resuspended in 0.5 ml RLT buffer (Qiagen GmbH, Hilden, Germany) supplemented with 1% mercaptoethanol (Riedel-deHaën, Hannover, Germany) and transferred to a glass tube. Acid-washed glass beads (Ø 0.45–0.55 mm, Merck, Darmstadt, Germany) were added up to the meniscus and the cells were disrupted by heavy vortexing three times for 3 min. After addition of 3.3 ml RLT buffer, the lysate was recovered with a glass capillary. Total RNA was isolated using the RNeasy Midi Kit (Qiagen AG, Basel, Switzerland) according to the manufacturer's protocol. RNA quality was assessed on an agarose gel. $Poly(A)^+$ RNA was amplified and biotin-labeled as follows. Starting with 20 μg total RNA, double-stranded cDNA was constructed using the GibcoBRL Superscript choice system (Life Technologies AG, Basel, Switzerland) and a T7-(T)24 primer to introduce a T7 promoter. Double-stranded cDNA was purified by three successive phenol:chloroform:isoamyl alcohol extractions and a subsequent alcohol precipitation. Phase-Lock Gel (5 Prime to 3 Prime, Boulder, CO) was used for all organic extractions to increase recovery. Using ~0.2–0.5 μg cDNA as a template, a biotin-labeled riboprobe was synthesized with the help of the T7 Megascrip system (Ambion, Austin, TX) and two biotin-labeled nucleotides (Bio-11-CTP and Bio-16-UTP, Enzo Diagnostics, Farmingdale, NY), which replaced one third of the provided CTP and UTP. The 6-h in vitro transcription reaction yielded ~50 μg cRNA, which was purified by RNA affinity resin (RNeasy spin columns, Qiagen). An aliquot was separated on a 0.8% agarose gel to check sample integrity. Subsequently, 40 μg of the transcript were used to hybridize a set of four commercially available oligonucleotide expression arrays (GeneChip Ye6100 arrays, Affymetrix, Santa Clara, CA) comprising a total of more than 260,000 oligonucleotides complementary to 6218 yeast open reading frames (ORFs). The biotinylated cRNA samples were fragmented to increase hybridization efficiency and specificity and to reduce potential problems caused by nucleic acid secondary structure (Wodicka *et al.*, 1997). Chip hybridization, washing, and staining with a streptavidin-phycoerythrin conjugate were performed using Affymetrix instrumentation according to the company's recommended protocols. The arrays were read at 7.5 μm with a confocal scanner (Molecular Dynamics, Sunnyvale, CA) and analyzed with GENECHIP software, version 3.0. A threshold of 20 arbitrary fluorescence units was assigned to any gene with a calculated expression level below 20, because discrimination of mRNA levels in this low range could not be performed. Chip hybridization and mRNA quality were verified with controls on the arrays consisting of 3′, middle, and 5′ regions of housekeeping genes (actin, SPT15, SRB4) and marker oligonucleotides at the corners, edges, and in the middle of the array (Wodicka *et al.*, 1997; unpublished data).

Statistical Analysis of the AFB_1/DMSO Data Set

mRNA levels were expressed as the average difference of hybridization signals, measured as fluorescence intensity, between perfect match and central-mismatch oligonucleotide probe sets (Wodicka *et al.*, 1997), and supplemented with an absent/present call generated by the Affymetrix software. Data from different chips were normalized using the parameter of total chip

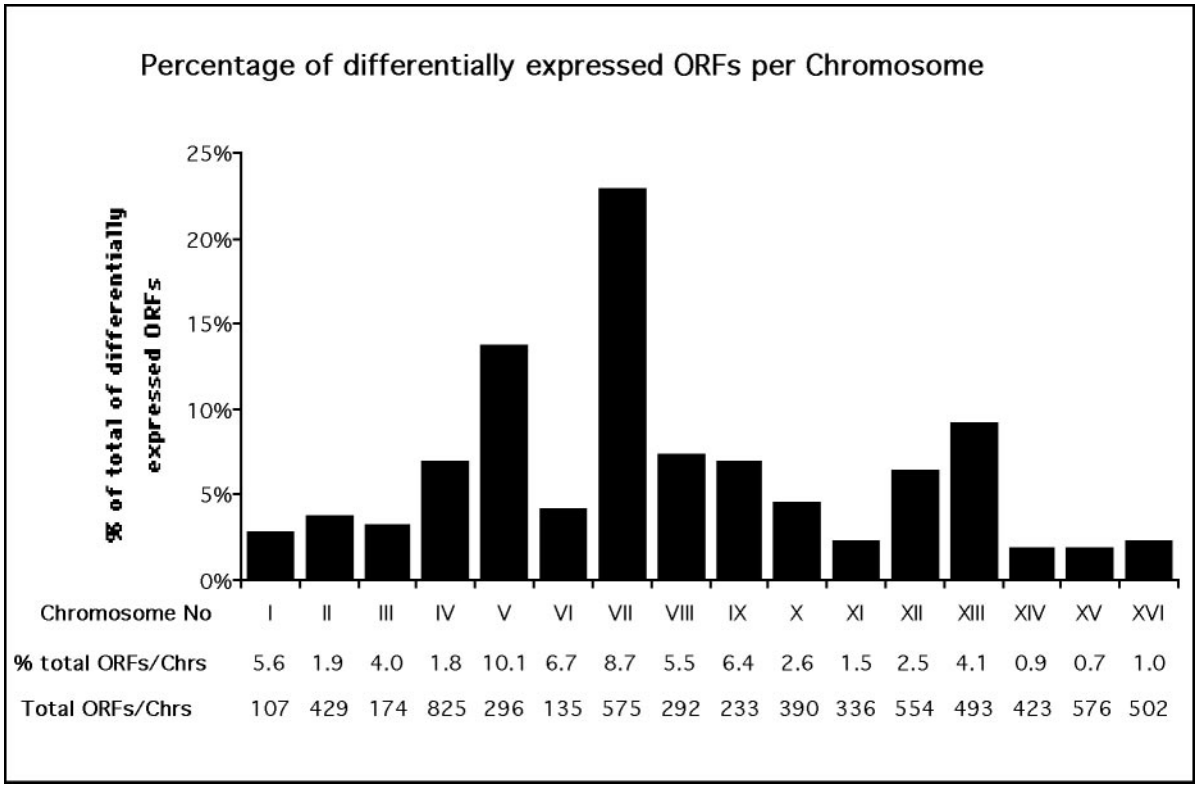

Figure 1. Distribution of AFB_1 responsive genes on the different chromosomes. Bars indicate the percentage of the total number of ORFs showing a ≥3-fold altered expression level; the roman numerals indicate the chromosome number. Information about the total ORF number of each chromosome (total ORFs/chrs) were retrieved from the MIPS database (Mewes *et al.*, 1997) and used to calculate the percentage of transcriptionally responsive ORFs per total number ORFs on each chromosome (% total ORFs/chrs). Data are means of two independent experiments.

signal. We calculated the mean of the average differences of two chips each of AFB_1 (AFB_1+) and solvent (AFB_1-) exposed cells. Only ORFs deviating <40% of this mean value (purity ≥ 0.6) were used for further analysis; 5630 ORFs fulfilled this criterion. The data sets were then imported into a MS Excel spreadsheet for further calculations and logical operations.

Preparation of RNA for Quantitative PCR Analysis

RNA was extracted from control cells, and cells were exposed to AFB_1 (Shirra *et al.*, 2001). RNA quality was assessed on a 0.8% agarose gel. DNaseI (0.05 U/ml, BD Biosciences, San Diego, CA) was added to ensure that no DNA was present in the extraction and after digestion at 37°C for 30 min, was inactivated in 1 mM EDTA (pH. 8.0). After extraction in phenol:chloroform:isoamyl alcohol (25:24:1, pH 4.5) and chloroform extraction, the aqueous layer was precipitated in 0.2 M NaOAc, 70% EtOH. The RNA pellet was then resuspended in TrisEDTA. One milligram of RNA was used for the reverse transcription reaction (first-strand cDNA synthesis), using a protocol described in the reverse transcription system kit (Promega, Madison, WI). cDNA was measured in a iCycler (Bio-Rad, Richmond, CA) by quantitative PCR (QPCR) using the IQ Green SYBR supermix kit (Bio-Rad). Cycle conditions included denaturation at 95°C, followed by 35 cycles of 95°C denaturation, 57°C reannealing, and 72°C reaction; a 95°C denaturation step; and a 55°C reannealing step. Rad51 cDNA was measured using oligos 5′-CAACTTGGGCGACCACTT G-3′ and 5′-AAAGGCTGGCCGACCAAT-3′. Act1 cDNA was measured using oligos 5′-CCACCAATCCAGACGGAGACT-3′ and 5′-GCCGAAAGAATG CAAAAG GA-3′. Rad1 cDNA was measured using 5′-CTAATTGTGCCTCATCGACCAA-3′ and 5′-GGATGCCAATAAACCGTCAGTATC-3′.

Measurements of DNA Damage–associated Recombination Frequencies in Checkpoint and **rad** *Mutants and in Wild Type*

We measured the frequency AFB_1, EMS, and BaP-DHD–associated translocations and drug toxicity in the *rad* mutants, YB195pSB229 (*rad51*) and YB150pCS512 (*rad1*); checkpoint mutants, YB324pCS316 (*sml1*, *mec1*) and YB325pCS316 (*mec1*); and the Rad^+ proficient strain YB110pCS316, as previously described (Sengstag *et al.*, 1996). YB195, YB150, YB324, and YB325 transformants were grown in YM His-Ade-Trp-Lys and YB110 transformants in YM His-Ade-Trp. After exposure to chemical agents, cells were resuspended to a density of 8×10^8 cells/ml, 100–250 μl was plated directly on YM Ade-Ura-Trp-Leu-Lys to select for His^+ recombinants, and the appropriate dilution was plated on YPD to measure viability. Selection plates were incubated at 30°C, and the colonies were counted after 7 days.

Chemicals

Benzo-(*a*)-pyrene-7,8-dihydrodiol (BaP-DHD; Midwest Research Institute, Kansas City, MO) and aflatoxin B_1 (AFB_1, Fluka, Buchs, Switzerland) were dissolved in DMSO. Ethyl-methane-sulfonate (EMS) was obtained from Eastman Kodak (Rochester, NY). DNA modifying enzymes were obtained from New England Biolabs, Inc. (Beverly, MA), 5-fluoroorotic acid (FOA) from Toronto Research Chemicals Inc. (Toronto, Ontario, Canada) and zymolyase was purchased from Seikagaku Corp. (Tokyo, Japan).

RESULTS

Genes responsive to AFB_1 treatment were identified through parallel analysis of the mRNA expression profiles. Cells from strain YMK2181pMK637 were treated for 4 h with either 25 μM AFB_1, the solvent DMSO, or water. $Poly(A)^+$ RNAs were amplified and labeled to make biotin-labeled cRNA probes. After hybridization to the chip arrays, the biotinylated probes were fluorescently labeled and the chips were read in a specially designed confocal scanning fluorescence microscope. The quantitative image analysis was based on the average of the differences between the perfect match oligonucleotide and the corresponding central-mismatch oligonucleotide so that nonspecific and background contributions could be eliminated. Each experiment was

Table 1. Yeast genes induced at least 3-fold upon AFB_1 exposure compared to control (DMSO)

Database ID[a]	Gene[b]	Ratio[c]	Intensity[d] DMSO	Intensity[d] AFB_1	Function[e]
Metabolism					
ypl123c	0	28.7	22	632	Ribonuclease of the T2 family
yer170w*	*ADK2*	5.1	20	102	Adenylate kinase, mitochondrial
ynl264c	0	4.9	20	97	Involved in lipid biosynthesis and multidrug resistance, similarity to Sec14p
ymr205c*	*PFK2*	4.1	20	81	6-phosphofructokinase, beta subunit
ymr217w	*GUA1*	3.7	20	74	GMP synthase (glutamine-hydrolysing)
ylr056w	*ERG3*	3.7	36	133	C-5 sterol desaturase
yhr003c	0	3.5	20	69	Similarity to molybdopterin-converting factor homolog YKL027w
ygr170w	*PSD2*	3.4	20	67	Phosphatidylserine decarboxylase 2
yil085c*	*KTR7*	3.4	20	67	Putative mannosyltransferase of the KRE2 family
yil134w*	*FLX1*	3.4	20	67	FAD carrier protein (MCF), mitochondrial
ygr287c	0	3.3	20	66	Similarity to maltase
ygr286c	*BIO2*	3.2	20	63	Biotin synthetase
yll061w*	0	3.1	33	102	High affinity *s*-methylmethionine permease, similarity to Gap1p and other amino acid permeases
ydl049c	*KNH1*	3.1	21	64	Functional homolog of KRE9
Energy					
yhr039c	*MSC7*	4.9	20	97	H^+-transporting ATPase V0 domain 13-kDa subunit, vacuolar
ygl119w*	*ABC1*	4.2	20	83	Ubiquinol-cytochrome-c reductase complex assembly protein
ymr205c*	*PFK2*	4.1	20	81	6-phosphofructokinase, beta subunit
Cell growth, cell division, and DNA Synthesis					
yer149c	*PEA2*	19.6	20	391	Involved in oriented growth toward mating partner
yhr152w	*SPO12*	8.5	20	169	Sporulation protein required for chromosome division in meiosis I
ygr152c	*RSR1*	8.2	20	163	GTP-binding protein of the ras superfamily
yer095w*	*RAD51*	7.7	29	224	DNA repair protein
ygr140w	*CBF2*	6.6	20	132	Kinetochore protein complex CBF3, 110-kDa subunit
yer016w*	*BIM1*	6.2	20	124	Associated with microtubules, required for a cell cycle check point
ycr089w	*FIG2*	5.5	20	109	Involved in mating induction
yer170w*	*ADK2*	5.1	20	102	Adenylate kinase, mitochondrial
yer111c*	*SWI4*	5.1	20	101	Transcription factor
ykl079w*	*SMY1*	5.0	20	99	Kinesin-related protein
ydl102w*	*CDC2*	5.0	21	104	DNA-directed DNA polymerase delta, catalytic 125-kDa subunit
ygl043w*	*DST1*	4.6	20	91	TFIIS (transcription elongation factor); DNA strand transfer protein catalyzing homologous DNA strand exchange
yar007c	*RFA1*	4.6	20	91	DNA replication factor A, 69-kDa subunit, binds ssDNA
ybr114w*	*RAD16*	4.5	38	169	Nucleotide excision repair protein
ymr167w	*MLH1*	4.1	20	82	DNA mismatch repair protein
yer122c*	*GLO3*	4.1	20	82	Zinc finger protein
ygr041w	*BUD9*	4.0	20	79	Budding protein
yhr135c*	*YCK1*	3.8	120	452	Casein kinase I isoform
yhl024w	*NOS1*	3.7	20	74	Required for sporulation and formation of meiotic spindle
ygl086w	*MAD1*	3.7	20	73	Spindle assembly checkpoint protein; required for cell cycle delay in response to impaired kinetochore function
yhr066w	*SSF1*	3.4	21	71	Mating protein
yjl098w	*SAP185*	3.3	20	66	Sit4p-associating protein
yfr036w*	*CDC26*	3.1	35	108	Anaphase-promoting complex (cyclosome) subunit
yer125w*	*RSP5*	3.1	40	123	Hect domain E3 ubiquitin-protein ligase
Transcription					
yer111c*	*SWI4*	5.1	20	101	Transcription factor
ykl139w	*CTK1*	4.7	20	93	Carboxy-terminal domain (CTD) kinase, alpha subunit
ygl043w*	*DST1*	4.6	20	91	TFIIS (transcription elongation factor)
yer171w*	*RAD3*	4.6	20	91	DNA helicase
yer122c*	*GLO3*	4.1	20	82	Zinc finger protein
ygr249w*	*MGA1*	3.9	20	78	Similarity to heat shock transcription factors
yer146w	*LSM5*	3.8	20	75	Similarity to human snRNP E
ynl251c	*NRD1*	3.7	20	74	Involved in regulation of nuclear pre-mRNA abundance
ygr246c	*BRF1*	3.5	20	70	TFIIIB subunit, 70 kDa
ymr112c	*MED11*	3.5	20	69	Mediator complex subunit
ygl172w	*NUP49*	3.3	20	66	Nuclear pore protein
ygl092w*	*NUP145*	3.3	20	65	Nuclear pore protein
ygl237c*	*HAP2*	3.2	48	154	CCAAT-binding factor subunit
yil130w	0	3.1	20	62	Similarity to Put3p and to hypothetical protein YJL206c
Protein synthesis					
ygr094w*	*VAS1*	8.1	20	161	Valyl-tRNA synthetase
yhr020w	0	3.3	20	66	Similarity to prolyl-tRNA synthetases; putative class II tRNA synthetase

(continues)

Table 1. (Continued)

Database ID[a]	Gene[b]	Ratio[c]	Intensity[d] DMSO	Intensity[d] AFB_1	Function[e]
Protein destination					
yer098w	*UBP9*	7.4	20	148	Ubiquitin carboxyl-terminal hydrolase
ylr163c	*MAS1*	5.0	20	99	Mitochondrial processing peptidase
ygl119w*	*ABC1*	4.2	20	83	Ubiquinol-cytochrome-c reductase complex assembly protein
yil085c*	*KTR7*	3.4	20	67	Putative alpha-1,2-mannosyltransferase
ymr264w	*CUE1*	3.2	20	64	Involved in ubiquitination and degradation at the ER surface
yfr036w*	*CDC26*	3.1	35	108	Subunit of anaphase-promoting complex (cyclosome)
yer125w*	*RSP5*	3.1	40	123	Hect domain E3 ubiquitin-protein ligase
Transport facilitation					
yjr040w*	*GEF1*	5.0	20	99	Voltage-gated chloride channel protein
yil134w*	*FLX1*	3.4	20	67	FAD carrier protein (MCF), mitochondrial
yhr175w*	*CTR2*	3.1	20	62	Copper transport protein
yll061w*	0	3.1	33	102	Similarity to amino acid transport protein Gap1p, MFS
Intracellular transport					
ygr257c	0	6.3	20	126	Similarity to members of the mitochondrial carrier family
yjr040w*	*GEF1*	5.0	20	99	Voltage-gated chloride channel protein
ykl079w*	*SMY1*	5.0	20	99	Kinesin-related protein
yor034c	*AKR2*	4.6	25	116	Involved in constitutive endocytosis of Ste3p
yhr135c*	*YCK1*	3.8	120	452	Casein kinase I isoform
ygl137w	*SEC27*	3.4	20	68	Coatomer complex beta′ chain (beta′-cop) of secretory pathway vesicles
yil134w*	*FLX1*	3.4	20	67	FAD carrier protein (MCF), mitochondrial
ygl172w*	*NUP49*	3.3	20	66	Nuclear pore protein
ygl092w*	*NUP145*	3.3	20	65	Nuclear pore protein
yhr175w*	*CTR2*	3.1	20	62	Copper transport protein
Cellular biogenesis					
yer016w*	*BIM1*	6.2	20	124	Associated with microtubules
Cell rescue, defense, cell death, and aging					
yer095w*	*RAD51*	7.7	29	224	DNA repair protein
yer171w*	*RAD3*	4.6	20	91	DNA helicase
ybr114w*	*RAD16*	4.5	38	169	Nucleotide excision repair protein
ydl102w*	*CDC2*	5.0	21	104	DNA polymerase delta, catalytic 125-kDa subunit
ygr138c*	0	4.1	20	81	Member of major facilitator superfamily (MFS) multidrug-resistance protein family
ygr249w*	*MGA1*	3.9	20	78	Similarity to heat shock transcription factors
yhr135c*	*YCK1*	3.8	120	452	Casein kinase I isoform
yor009w	0	3.7	53	195	Similarity to Tir1p and Tir2p
yer143w	*DDI1*	3.6	20	71	Induced in response to DNA alkylation damage
yer125w*	*RSP5*	3.1	40	123	Hect domain E3 ubiquitin-protein ligase
Ionic homeostasis					
yjr040w*	*GEF1*	5.0	20	99	Voltage-gated chloride channel protein
yhr175w*	*CTR2*	3.1	20	62	Copper transport protein
Classification not yet clear-cut					
yel055c	*POL5*	6.2	20	124	DNA polymerase V
yar050w*	*FLO1*	4.4	20	88	Flocculin, cell wall protein involved in flocculation
ycl068c	0	3.1	20	61	Similarity to the N-terminal third of Bud5p
ygl179c	0	3.0	20	60	Serine/threonine protein kinase with similarity to Elm1p and Kin82p
Unclassified					
yel068c	0	35.1	20	701	Protein of unknown function
ygr107w	0	17.6	20	351	Protein of unknown function
ygr164w	0	16.0	20	320	Similarity to *Hansenula wingei* mitochondrial site-specific nuclease Pir
ygr247w	0	15.4	60	923	Protein of unknown function
ygr153w	0	10.5	20	209	Protein of unknown function
ygr176w	0	10.4	31	321	Protein of unknown function
yfl012w	0	9.9	20	197	Protein of unknown function
yel025c	0	8.1	20	161	Protein of unknown function
ygr203w	0	6.7	20	134	Similarity to *X. laevis* protein-tyrosin-phosphatase Cdc homolog 2 and to hypothetical protein YPR200c
yhr217c	0	6.1	20	121	Similarity to subtelomeric encoded YDR544c
yer189w	0	5.9	20	117	Similarity to subtelomerically-encoded proteins including Yil177p, Yhl049p, and Yjl225p
yil102c	0	5.4	20	107	Similarity to YIL014c-a
ydr149c	0	5.0	20	100	No annotation
yal037w	0	4.6	21	97	Similarity to GTP-binding proteins

(continues)

Table 1. (Continued)

Database ID[a]	Gene[b]	Ratio[c]	Intensity[d] DMSO	Intensity[d] AFB_1	Function[e]
yer038c	0	4.6	20	92	Protein of unknown function
yor059c	0	4.5	55	245	Similarity to YGL144c
yjl100w	0	4.4	20	88	Similarity to hypothetical *C. elegans* protein C56A3.8
ygr150c	0	4.4	20	87	Similarity to Yjl083p
yil007c	0	4.4	20	87	Similarity to human proteosomal modulator subunit p27
yer037w	0	4.3	23	99	Similarity to hypothetical protein YGL224c
ygr081c	0	4.3	22	95	Similarity to chicken myosin heavy chain Pir
ygl246c	0	4.1	20	82	Similarity to *C. elegans* dom-3 protein
yfl060c	*SNO3*	4.1	20	81	Member of stationary phase-induced gene family
ydl105w	*QRI2*	4.1	20	81	Protein of unknown function
ygl102c	0	3.9	28	110	Protein of unknown function
ylr181c	0	3.8	20	76	Protein of unknown function
yil040w	0	3.8	20	75	Similarity to *T. brucei* NADH
yer104w	0	3.8	20	75	Protein of unknown function
yjl104w	0	3.7	24	89	Similarity to *C. elegans* hypothetical protein F45G2.c
ybr013c	0	3.7	20	74	Protein of unknown function
ygl131c	0	3.7	22	81	Similarity to *S. pombe* hypothetical protein C3H1.12C
ygr126w	0	3.6	20	72	Similarity to hypothetical protein YPR156c
yjl109c	0	3.6	20	72	Similarity to ATPase Drs2p
yjr038c	0	3.6	20	71	Protein of unknown function
ygl079w	0	3.5	83	290	Protein of unknown function
yil019w	0	3.4	20	67	Has potential coiled-coil region, similarity to *S. pombe* hypothetical protein SPAC3F10
ygl057c	0	3.3	25	82	Protein of unknown function
yel057c	0	3.2	40	129	Protein of unknown function
ylr003c	0	3.2	20	64	Protein of unknown function
ygl133w	0	3.1	20	62	Similarity to hypothetical protein YPL216w
ypl146c	0	3.1	20	62	Similarity to myosin heavy chain proteins
ycr013c	0	3.1	20	62	Similarity to *M. leprae* B1496_F1_41 protein
ymr255w	0	3.1	123	380	Protein of unknown function
ybr250w	0	3.1	20	61	Protein of unknown function
yfr013w	0	3.1	20	61	Similarity to YOL017w
ydl039c	0	3.0	73	221	Protein of unknown function
yfr024c	0	3.0	20	60	Similarity to Ysc84p, Rvs167p, Abp1p, and Sla1p
ykr088c	0	3.0	20	60	Similarity to *B. subtilis* spore germination protein II

[a] Indicates ORF number, and the asterisk (*) indicates ORFs that fall into multiple categories.

[b] 0 indicates no designation.

[c] Ratio is respective to cells treated without toxin.

[d] Hybridization signal given in arbitrary units of fluorescence studies.

[e] Description of gene function according to the Yeast Protein Database.

done in duplicate. After normalization of the data, the fold change in the transcriptional expression of each ORF was calculated using the AFB_1 exposed (AFB_1+) and control (AFB_1-) data sets. Differences in hybridization intensity between the same ORFs are proportional to changes in transcript levels, and the intensity changes >2.0-fold are both significant and accurate, according to previous studies (Wodicka *et al.*, 1997). Comparison of the data sets of 0.4% DMSO and H_2O-treated cells identified one ORF whose expression was influenced by the solvent 0.4% DMSO; 478 specific ORFs exhibited greater than twofold change in expression due to AFB_1 exposure. Chromosomal distribution of the responsive ORFs is depicted in Figure 1. Nearly one fourth of all the responsive genes are located on chromosome VII, where they represent 8.7% of the ORFs.

Of 6218 ORFs, 183 (2.9%) showed at least a threefold change in transcript levels after AFB_1 exposure. One hundred seventeen were upregulated; the strongest induction was 35.1-fold (YEL068C; Table 1). Of the 66 genes that were downregulated, the strongest repression was 14.1-fold (YDR306C; Table 2). Most of the products of the responsive genes are located in the nucleus (79%; Figure 2). To gain an overview of the transcriptional response to AFB_1, the ORFs were assigned to functional categories according to the MIPS database (Munich Information Center for Protein Sequences; Mewes *et al.*, 1997). The category of cell growth, cell division, and DNA synthesis contains 30 AFB_1-responsive genes, the most number of any category. The second most numerous is the metabolism category, which contains 28 AFB_1-responsive genes. However, comparing the percentage of responsive genes in each respective category, the category of cell rescue, defense, cell death, and aging contains the largest percentage of AFB_1-responsive genes (4.8%; Figure 2). A more detailed view is provided by the analysis of the subcategories (Figure 3). Thus, there are genes in several functional categories whose expression is either induced or repressed after AFB_1 exposure.

Because the genotoxicity of AFB_1 may result from AFB_1-induced DNA damage, we identified AFB_1-inducible DNA repair genes. Of 109 genes involved in DNA damage repair according to the Yeast Protein Database (Payne and Garrels, 1997), 15 (14%) were upregulated (*RAD51, CDC2(POL3),*

Table 2. Yeast genes repressed at least 3-fold upon AFB_1 exposure compared to control (DMSO)

Database ID[a]	Gene[b]	Ratio[c]	Intensity[d] DMSO	Intensity[d] AFB_1	Function[e]
Metabolism					
yil154c*	*IMP2*	−6.4	127	20	Involved in control of mitochondrial sugar utilization
ykl174c*	0	−4.1	82	20	Similarity to choline transport protein Hnm1p
yer052c	*HOM3*	−3.9	77	20	L-aspartate 4-P-transferase
yil116w	*HIS5*	−3.9	77	20	Histidinol-phosphate aminotransferase
yer061c*	*CEM1*	−3.8	76	20	Beta-keto-acyl-ACP synthase, mitochondrial
yjl068c	0	−3.8	75	20	Similarity to human esterase D
ymr296c	*LCB1*	−3.7	74	20	Serine C-palmitoyl transferase subunit
ygr124w	*ASN2*	−3.6	71	20	Asparagine synthetase
yhr092c*	*HXT4*	−3.5	69	20	Moderate- to low-affinity glucose transporter, MFS
ydr242w	*AMD2*	−3.4	87	26	Amidase
ygl186c*	0	−3.3	103	31	Member of the purine/cytosine permease family, MFS
yml070w*	*DAK1*	−3.3	76	23	Putative dihydroxyacetone kinase
ylr240w*	*VPS34*	−3.3	65	20	Phosphatidylinositol 3-kinase
yhr106w	*TRR2*	−3.2	63	20	Thioredoxin reductase
yer061c*	*CEM1*	−3.8	76	20	Beta-keto-acyl-ACP synthase, mitochondrial
Cell growth, cell division, and DNA synthesis					
yhr165c*	*PRP8*	−5.2	104	20	U5 snRNP protein, pre-mRNA splicing factor
yel032w	*MCM3*	−3.9	77	20	Replication initiation protein
yil047c*	*SYG1*	−3.9	77	20	Member of the major facilitator superfamily (MFS)
ybl105c*	*PKC1*	−3.9	77	20	Serine/threonine protein kinase
ycr088w	*ABP1*	−3.7	74	20	Actin-binding protein
ygl073w*	*HSF1*	−3.7	73	20	Heat shock transcription factor
Transcription					
ylr357w*	*RSC2*	−5.2	104	20	Component of abundant chromatin remodeling complex
yhr165c*	*PRP8*	−5.2	104	20	U5 snRNP protein, pre-mRNA splicing factor
ygl013c*	*PDR1*	−3.7	74	20	Transcription factor related to Pdr3p
ygl073w*	*HSF1*	−3.7	73	20	Heat shock transcription factor
ycl031c*	*RRP7*	−3.2	96	30	Involved in pre-rRNA processing and ribosome assembly
ymr219w	*ESC1*	−3.1	279	91	Establishes silent chromatin
ybr237w*	*PRP5*	−3.0	73	24	Pre-mRNA processing RNA-helicase
yjr017c	*ESS1*	−3.0	136	45	Processing/termination factor 1
Protein synthesis					
yer117w	*RPL23B*	−3.6	83	23	Ribosomal protein L23.e
ycl031c*	*RRP7*	−3.2	96	30	Involved in pre-rRNA processing and ribosome assembly
Protein destination					
ymr197c*	*VTI1*	−12.2	243	20	V-SNARE: involved in Golgi retrograde protein traffic
ybr283c	*SSH1*	−8.6	171	20	Involved in co-translational pathway of protein transport
ylr121c	*YPS4*	−4.6	185	40	Yapsin 4, Gpi-anchored aspartyl protease
ygr028w*	*MSP1*	−4.6	91	20	Intra-mitochondrial sorting protein, ATPase
ycl031c*	*RRP7*	−3.2	96	30	Involved in pre-rRNA processing and ribosome assembly
ybr237w*	*PRP5*	−3.0	73	24	Pre-mRNA processing RNA-helicase
ybr201w	*DER1*	−3.0	60	20	Involved in protein degradation in the ER
Transport facilitation					
yil088c	0	−4.8	96	20	Similarity to members of the major facilitator superfamily (MFS)
yll055w	0	−4.5	107	24	Similarity to Dal5p and members of the allantoate permease family, MFS
ykl174c*	0	−4.1	82	20	Similarity to choline transport protein Hnm1p
yhr092c*	*HXT4*	−3.5	69	20	Moderate- to low-affinity glucose transporter, MFS
ygl186c*	0	−3.3	103	31	Member of the purine/cytosine permease family, MFS
Intracellular transport					
ymr197c*	*VTI1*	−12.2	243	20	V-SNARE: involved in Golgi retrograde protein traffic
yil115c	*NUP159*	−5.2	103	20	Nuclear pore protein
ygr028w*	*MSP1*	−4.6	91	20	Intra-mitochondrial sorting protein, ATPase
ymr183c	*SSO2*	−3.8	76	20	Syntaxin (T-SNARE)
yhr092c*	*HXT4*	−3.5	69	20	Moderate- to low-affinity glucose transporter, MFS
ylr240w*	*VPS34*	−3.3	65	20	Phosphatidylinositol 3-kinase
ydr246w	*TRS23*	−3.2	131	41	Involved in targeting and fusion of ER to golgi transport vesicles
yhr156c	0	−3.2	64	20	Weak similarity to mouse kinesin KIF3B
ycr032w	*BPH1*	−3.2	63	20	Probably involved in acetic acid export
Cellular biogenesis					
yil154c*	*IMP2*	−6.4	127	20	Involved in control of mitochondrial sugar utilization
ylr357w*	*RSC2*	−5.2	104	20	Component of abundant chromatin remodeling complex
Cellular communication/signal transduction					
yil047c*	*SYG1*	−3.9	77	20	Member of the major facilitator superfamily (MFS)
ybl105c*	*PKC1*	−3.9	77	20	Serine/threonine protein kinase
ylr240w*	*VPS34*	−3.3	65	20	Phosphatidylinositol 3-kinase

(continues)

Table 2. (Continued)

Database ID[a]	Gene[b]	Ratio[c]	Intensity[d] DMSO	Intensity[d] AFB_1	Function[e]
Cell rescue, defense, cell death and aging					
ymr173w	*DDR48*	−4.9	98	20	Heat shock protein, ATPase, Chaperon
yhl046c	0	−3.9	78	20	Similarity to members of the Srp1p/Tip1p family
ybl105c*	*PKC1*	−3.9	77	20	Serine/threonine protein kinase
ygl013c*	*PDR1*	−3.7	74	20	Transcription factor
ygl073w*	*HSF1*	−3.7	73	20	Heat shock transcription factor
yml070w*	*DAK1*	−3.3	76	23	Putative dihydroxy acetone kinase
Unclassified					
ydr306c	0	−13.1	281	20	Contains an f-box, weak similarity to *S. pombe* hypothetical protein SPAC6F6
ypl247c	0	−5.4	262	49	Similarity to human HAN11 protein and petunia an11 protein
yal031c	*FUN21*	−5.2	103	20	Protein of unknown function
ygr102c	0	−5.1	102	20	Protein of unknown function
ymr115w	0	−4.6	91	20	Similarity to YKL133c
yfl043c	0	−4.4	87	20	No annotation
ydr229w	0	−4.2	137	33	Protein of unknown function, possible coiled-coil protein
yil087c	0	−4.0	121	30	Protein of unknown function
yil077c	0	−4.0	79	20	Protein of unknown function
yml067c	0	−3.6	72	20	Similarity to YAL042w
ybr137w	0	−3.5	84	24	Protein of unknown function
ydl076c	0	−3.5	77	22	Protein of unknown function
ygl045w	0	−3.5	69	20	Protein of unknown function
yhr090c	*NBN1*	−3.4	68	20	Protein with effect on bem and rad phenotypes, similarity to YOR064c, YNL097c
ydr128w	0	−3.3	66	20	Similarity to Sec27p, YMR131c and human retinoblastoma-binding protein
ykl204w	0	−3.3	66	20	Protein of unknown function, probable purine nucleotide-binding protein
ygl082w	0	−3.3	69	21	Similarity to hypothetical protein YPL191c
ypl170w	0	−3.2	85	27	Similarity to *C. elegans* LIM homeobox protein
ypr063c	0	−3.2	63	20	Protein of unknown function
ygl005c	0	−3.1	61	20	Similarity to *X. laevis* kinesin-related protein Eg5
ymr184w	0	−3.0	60	20	Protein of unknown function
ycl044c	0	−3.0	60	20	Protein of unknown function

[a] Indicates ORF number, and the asterisk (*) indicates ORFs that fall into multiple categories.

[b] 0 indicates no designation.

[c] Ratio is respective to cells treated without toxin.

[d] Hybridization signal given in arbitrary units of fluorescence.

[e] Description of gene function according to the Yeast Protein Database.

DST1, RAD3, RSP5, RFA1, RAD16, MLH1, MMS21, DIN7, MET18, HPR5, RFA2, MSH6, RAD1) and 3 were repressed (*DDR48, SIR4, DNL4*) at least twofold. Furthermore, of the 16 genes assigned to specific repair pathways, 11 genes (69%) function in recombinational repair, 7 genes (44%) in nucleotide excision repair, and 4 genes function in both pathways. Only 2 of the repressed genes are not in either pathway but function in nonhomologous end joining (NHEJ; Table 3). Analysis of cell cycle periodicity of the repair genes showed that changes in expression levels after AFB_1 exposure are not simply caused by changes in cell cycle progression (Keller-Seitz, 2001). Furthermore, 44 genes exhibiting at least a twofold or greater change in expression are involved in damage signaling, stress response, or cell cycle control (Table 4). Thus, AFB_1 exposure induces DNA repair genes in NER, MMR, and recombinational DNA repair.

AFB_1-inducible repair genes that function in multiple recombination pathways include *RAD51* (7.7-fold increased) and *RAD1* (2.1-fold increased). We confirmed that *RAD51* RNA increases after AFB_1 exposure by QPCR, using actin RNA as a control (Figure 4). YB110 (pCS316) was exposed to 25 μm AFB_1 for 4 h, and RNA was extracted for QPCR. The amount of *RAD51* RNA increased fivefold in YB110 cells treated with AFB_1, whereas actin RNA did not significantly increase (Figure 4). However, we found that the amount of *RAD1* mRNA increased less than twofold (unpublished data). The differences between the QPCR results and the microarray results are likely due to the greater sensitivity of the microarrays (Etienne *et al.*, 2004).

Although we did not prove that the induced expression of the NER genes and *RAD51* is necessary for AFB_1-associated recombination, we did use *rad1* (YB150 pCS512) and *rad51* mutant (YB195 pSB229) yeast strains to determine whether *RAD1* or *RAD51* function in AFB_1-associated recombination and lethality (Figure 5). We measured the frequencies of AFB_1-associated translocations by selecting for His^+ recombinants as previously described (Fasullo and Davis, 1987). Besides AFB_1, the carcinogen benzo-(*a*)-pyrene-7,8-dihydrodiol (BaP-DHD) and the mutagen ethyl methanesulfonate (EMS) were also tested. Although the viability of both mutant strains is slightly decreased after exposure to AFB_1, the *rad51* strain is hypersensitive to EMS and the *rad1* strain is hypersensitive to BaP-DHD (Figure 5). Compared with the wild-type (Rad^+) strain, the frequency of AFB_1-associated

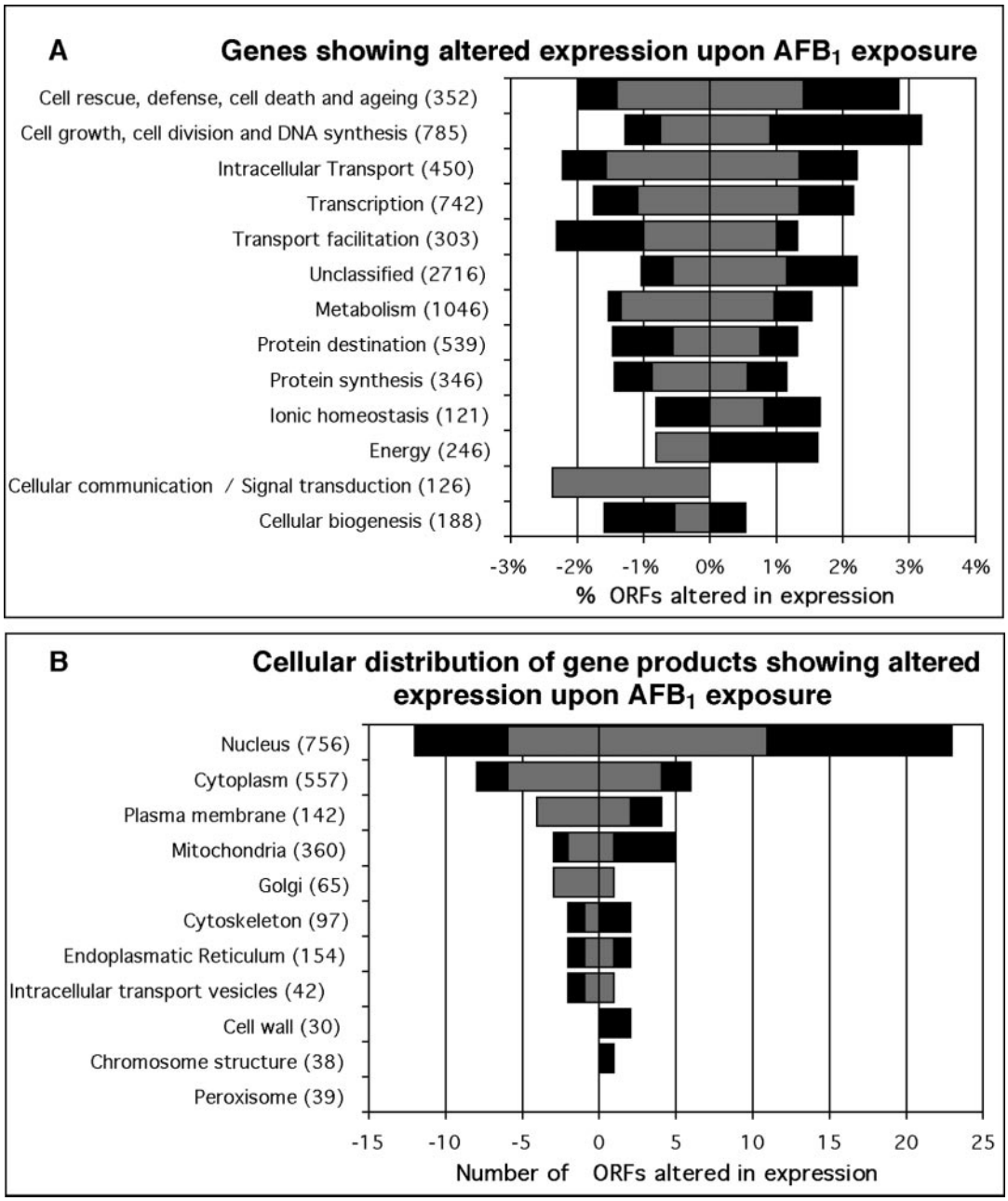

Figure 2. Functional (A) and cellular (B) classification of AFB_1 responsive ORFs. Indicated are transcripts levels altered more than threefold (gray bars) and fourfold (black bars) after 4-h treatment with 25 μM AFB_1. The amount of ORFs in the cellular distribution (B) is given as absolute numbers, and the ORFs per functional category (A) are given as percent of total genes assigned to the respective category. Categories are derived from the MIPS database (Mewes *et al.,* 1997). Note that some ORFs fall into multiple categories. Values are means of two independent experiments.

translocations was slightly decreased in both the *rad51* and *rad1* mutants, whereas the frequency of EMS-associated recombination increased in the *rad51* strain and the frequency of BaP-DHD–associated translocations was significantly higher in the *rad1* mutant (Figure 5). At EMS concentrations greater than 40 mM, EMS-associated recombination could not be measured because of the extreme EMS toxicity. Because the frequencies of spontaneous recombination are $(1.4 \pm 0.4) \times 10^{-7}$ and $(3.8 \pm 1.8) \times 10^{-8}$ in the wild-type and *rad1* strains, respectively, and low compared with the DNA damage–associated frequencies, the DNA damage–associated frequencies are similar to the net recombination frequencies. In the *rad51* mutant the spontaneous frequency (avg.) was $(1.3 \pm 0.2) \times 10^{-6}$, and thus the net recombination frequencies (avg.) for the highest level of AFB_1-associated, EMS-associated, and BaP-DHD–associated translocations were 3.4×10^{-6}, 96×10^{-6}, 7.7×10^{-6}, respectively. The highest net AFB_1-associated frequency is still ~25% lower in the *rad51* diploid than in wild-type, whereas the highest net BaP-DHD–associated frequency was about threefold higher in the *rad51* diploid than in wild type. These results indicate that *RAD51* and *RAD1* function in AFB_1-associated recom-

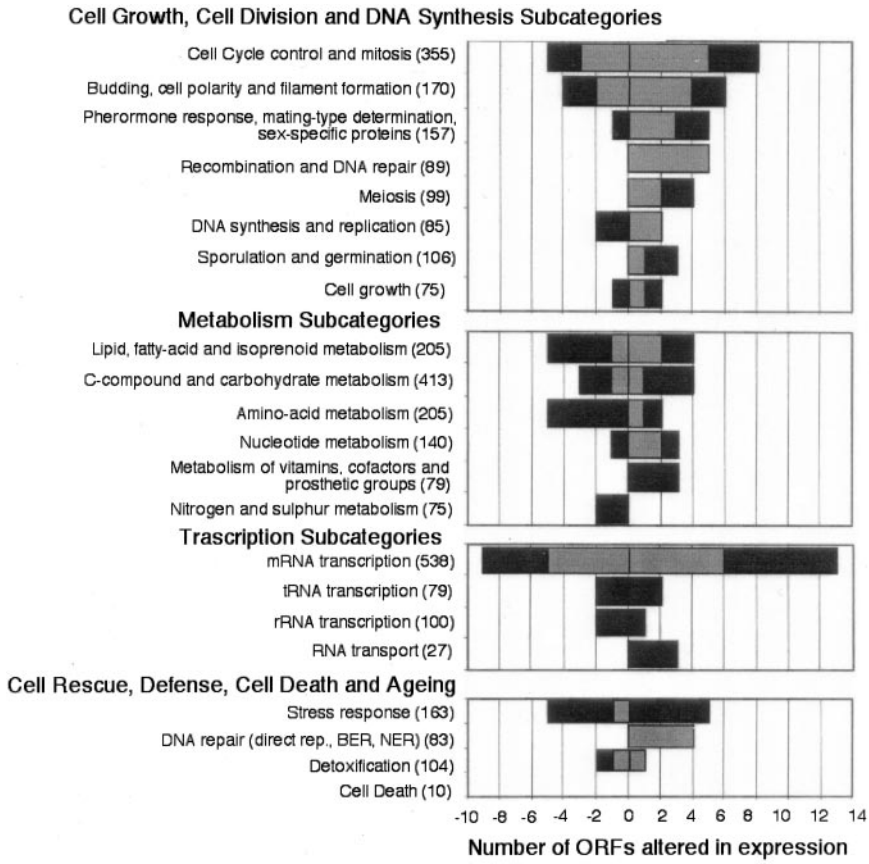

Figure 3. Assignments of AFB_1 responsive yeast genes to subcategories. Gray bars indicate ORFs showing an over threefold, black bars over fourfold change in expression. Categories and subcategories are derived from the MIPS database (Mewes *et al.,* 1997). Values are means of two independent experiments.

bination, whereas *RAD51* and *RAD1* suppress EMS-associated and BaP-DHD–associated recombination, respectively.

To further understand the correlation between *RAD51* expression and AFB_1-associated recombination, we measured translocation frequencies in *mec1* checkpoint strains. *mec1* checkpoint mutants are deficient in *RAD51* induction after MMS and x-ray exposure (Gasch *et al.,* 2001). We found that the *mec1-21* (YB325) and *mec1*Δ*::TRP1* (YB324) mutants cannot induce *RAD51* levels after exposure to 25 μM AFB_1 (Figure 4). The translocation frequency increased 26-fold after wild type (YB110 pCS316) was exposed to 25 μM AFB_1, consistent with previous studies (Sengstag *et al.,* 1996). We found no significant increase in translocation frequencies after both the *mec1* deletion mutant (YB324 pCS316) and the *mec1-21* mutant (YB325 pCS316) were exposed to 25 μM AFB_1 (Table 5). However, because the *sml1* null mutant exhibited a decrease in AFB_1-associated recombination, the decrease in AFB_1-associated recombination in the *mec1* null mutant could be partially conferred by the *sml1* mutation. To increase Rad51 in the *mec1-21* strain (YB325), we introduced the 2 μ *LEU2* plasmid (pR51.3; Sung and Stratton, 1996) containing *RAD51* expressed from a strong constitutive *PGK* (phosphoglycerol kinase) promoter by selecting for Leu^+ transformants. By QPCR, we found that the basal level of *RAD51* RNA before and after AFB_1 exposure in the Leu^+ transformants was the same and more than a thousand fold higher than the basal level of *RAD51* RNA in *mec1-21* (YB325), whereas there was no change in *ACT1* RNA levels (unpublished data). In YB325 (pR51.3) cells, translocation frequencies increased ninefold after AFB_1 exposure. *RAD51* overexpression in *mec1-21* also increased lethality after AFB_1 exposure, suggesting that other detrimental recombination events may also be generated. These data indicate that an increase in *RAD51* expression can enhance AFB_1-associated recombination in a strain deficient in the DNA damage inducibility of *RAD51*.

DISCUSSION

AFB_1 is a strong recombinagen but weak mutagen in *S. cerevisiae*. To elucidate the genotoxic properties of AFB_1, we investigated the global transcriptional response of a diploid yeast strain after exposure to AFB_1 using high-density oligonucleotide arrays. We determined the expression pattern of 6218 ORFs representing the entire yeast genome. Other studies have determined the global transcriptional responses after exposure to MMS and ionizing radiation; however, these studies have used haploid strains, rendering it difficult to compare data. Nonetheless, our results demonstrate that AFB_1 exposure elicits a complex transcriptional response pattern. A large fraction of the responsive genes are involved in cell rescue, cell cycle control, and DNA repair; this latter category included genes involved in both excision and recombinational repair. Subsequent comparison of survival and translocation frequencies in *rad51* and *rad1* mutants after exposure to AFB_1, EMS, and BaP-DHD indicate that the stimulation of recombination by different carcinogens requires different DNA repair genes.

The gene expression patterns reveal that AFB_1-induced transcripts are not evenly distributed among yeast chromosomes (Figure 1). The differences ranged from ≥3-fold induction of 10% of ORFs on chromosome V to only 0.7% on chromosome XV. On the level of individual ORFs, a subset of genes that exhibit significant change in expression are

Table 3. AFB_1-responsive DNA repair genes showing a 2-fold or greater change in expression

Gene name[a]	ORF	Ratio[b]	Intensity[c] DMSO	Intensity[c] AFB_1	NER[d]	RR[e]	Other pathways[f]	Function[g]
RAD51‡	YER095W	7.7	29	224		+		Stimulates pairing and strand-exchange between homologous ssDNA and dsDNA, functionally similar to *E. coli* recA protein
POL3	YDL102W	5.0	21	104	+		BER, MMR, TLS	DNA polymerase delta large subunit
DST1	YGL043W	4.6	20	91		+		TFIIS, DNA strand transfer protein catalyzing homologous DNA strand exchange
*RAD3**	YER171W	4.6	20	91	+	+		DNA helicase, component of TFIIH
RFA1†	YAR007C	4.6	20	91	+	+		DNA replication factor A, 69-kDa subunit
RAD16#†	YBR114W	4.5	38	169	+			DNA helicase involved in G2 repair of inactive genes, member of the Snf2 (Swi2) protein family, recognizes transition between paired and unpaired DNA strands
MLH1	YMR167W	4.1	20	82		+	MMR	MMR protein and homolog of *E. coli* mutL, shows anti-recombinase activity
MMS21	YEL019C	2.9	30	87		+		Involved in DNA repair
*MET18**	YIL128W	2.5	20	49	+			Involved in NER and RNA polymerase II transcription
HPR5‡#	YJL092W	2.4	59	140		+	TLS, NHEJ	DNA helicase involved in DNA repair; suppressor of RAD6 and RAD18, has anti-recombinase function
RFA2†	YNL312W	2.2	22	48	+	+		DNA replication factor A, 36-kDa subunit
MSH6	YDR097C	2.2	20	43		+	MMR	Part of DNA mismatch binding factor, involved in repair of single base mismatches
RAD1#†	YPL022W	2.1	20	41	+	+	MMR	Homolog of human XP-F and mammalian ERCC-4 protein, acts in different recombination pathway than Rad52p
MLH3	YPL164C	2.0	20	40		+	MMR	Interacts with Mlh1p and functions with Msh3p to suppress homologous recombination
SIR4	YDR227W	−2.1	47	22			NHEJ	Silencing regulatory and DNA-repair coiled-coil protein
DNL4	YOR005C	−2.0	42	21			NHEJ	ATP-dependent DNA ligase IV; involved in nonhomologous end joining

[a] Assignment to specific repair pathways according to Friedberg *et al.* (1995) and the Yeast Protein Database (YPD). The symbols *, #, ‡ and † indicate membership in the *RAD3*, *RAD6*, *RAD52* epistasis groups and NER repairosome, respectively.

[b] Ratio is respective to cells treated without toxin.

[c] Hybridization signal is given in arbitrary units of fluorescence.

[d] Nucleotide excision repair.

[e] Recombination repair.

[f] Other repair pathways include base excision repair (BER), mismatch repair (MMR), translesion synthesis (TLS) and non-homologous end-joining (NHEJ).

[g] Description of gene function according to the Yeast Protein Database.

closely linked; these include *RAD3* (YER171W, 4.6-fold increased), which is located between *ADK2* (YER170W, 5.1-fold increased) and *BRR2* (YER172C, 2.2-fold increased), and *RAD51* (YER095W, 7.7-fold increased), that is located close to *UBP9* (YER098W, 7.4-fold increased) and *SWI4* (YER111C, 5.1-fold increased). The linked ORFs are on different DNA strands (Goffeau *et al.*, 1996), suggesting that changes in chromosome structure may alter expression of multiple genes. Hence, our data suggest that some DNA damage responsive genes might be organized as clusters in coregulated chromosomal regions.

The complex response pattern caused by AFB_1 reflects the broad range of toxic effects in the cell; however, the pattern of gene expression after exposure to AFB_1 does not reflect a general stress response or a general response to DNA damaging agents, such as alkylating agents (Jelinsky and Samson, 1999). Five stress response genes, *DDR48*, *PAI3*, *YML131W*, *YKL100C*, and *YNL116W*, that are upregulated after MMS exposure (Jelinsky and Samson, 1999) and saline stress conditions (Posas *et al.*, 2000) are not induced after exposure to AFB_1. The only gene assigned to the general stress response that was induced with MMS (17.8-fold) and AFB_1 (2.6-fold) was the DNA damage-inducible gene *DDI1*. It is unlikely that the AFB_1 solvent DMSO triggered the general stress response, because the only difference between the gene expression patterns after exposure to DMSO and H_2O was the DMSO-dependent induction of YML131W. In addition, *RNR1*, which is generally induced after exposure alkylating agents and UV (Elledge and Davis, 1990), was not induced after exposure to AFB_1. We therefore suggest that the gene expression pattern of the cells exposed to AFB_1 did not result from a general stress response but from specific AFB_1-induced toxicity, such as AFB_1-induced DNA damage.

The gene expression patterns may provide further insights into the recombinogencity of AFB_1. Many of the responsive genes are directly or indirectly involved in recombination (reviewed in Aguilera *et al.*, 2000; Nicholson *et al.*, 2000). Several are also induced after diploid cells are exposed to γ rays; these include *RAD51*, *SRS2*, *RFA1*, *RFA2*, and *MSH6* (Mercier *et al.*, 2001). Among the AFB_1-inducible DNA repair genes, *RAD51* (7.7-fold increased) exhibited the strongest induction. The proteins encoded by the AFB_1-inducible genes *RFA1* and *RFA2* are subunits of the replication factor A (RPA) and promote Rad51-stimulated DNA pairing and strand exchange in vitro (Sung, 1994) by removing secondary DNA structures (Sung and Robberson, 1995).

Table 4. AFB_1-responsive genes involved in damage signaling, stress response, and cell cycle control.

Gene name	ORF[a]	Ratio[b]	Intensity[c] DMSO	Intensity[c] AFB_1	Function[d]
SPO12	YHR152W	8.5	20	169	Sporulation protein
RSR1	YGR152C	8.2	20	163	GTP-binding protein of the ras superfamily
CBF2	YGR140W	6.6	20	132	Subunit A of CBF3 kinetochore complex, required for cell cycle arrest at anaphase
BIM1	YER016W	6.2	20	124	Microtubules-associated protein
SWI4	YER111C	5.1	20	101	Transcription factor that participates in the SBF complex (Swi4p–Swi6p) for regulation at the cell cycle box (CCB) element
CTK1	YKL139W	4.7	20	93	Putative TOR downstream target, cyclin-dependent protein kinase that phosphorylates c-terminal domain of RNA polymerase II large subunit
GLO3	YER122C	4.1	20	82	GAP involved in transition from stationary to proliferative phase
MGA1	YGR249W	3.9	20	78	Similarity to heat shock transcription factor
YCK1	YHR135C	3.8	120	452	Casein kinase I isoform, 41% similarity to Hrr25p
?	YOR009W	3.7	53	195	Similarity to members of the PAU1 family, has stress-induced proteins SRP1/TIP1 family signature
MAD1	YGL086W	3.7	20	73	Involved in TOR signaling, DNA damage-induced recombination, required for cell cycle delay in response to impaired kinetochore function
DDI1	YER143W	3.6	20	71	Induced in response to DNA alkylation damage, gene contains a cis-acting element that regulates expression of MAG1
SAP185	YJL098W	3.3	20	66	Phosphatase Sit4p-associating protein, role in cell cycle control
CDC26	YFR036W	3.1	35	108	Subunit of anaphase-promoting complex, heat inducible
RSP5	YER125W	3.1	40	123	Ubiquitin-protein ligase, functions in the OLE1 activation pathway
CLB1	YGR108W	2.9	20	57	Cyclin, G2/M-specific
BIK1	YCL029C	2.7	22	59	Microtubule-associated protein required for microtubule function during mitosis and mating, interacts with Bim1p and Bub3p
RNH1	YMR234w	2.6	20	52	Ribonuclease H, endonuclease that degrades RNA in RNA-DNA hybrids
DIN7	YDR263C	2.5	20	50	DNA-damage inducible protein, production increases during meiosis at about the time of recombination, has similarity to human XPG protein (DNA-repair protein complementing XP-G cells) related to xeroderma pigmentosum group G and Cockayne's syndrome
PAK1	YER129W	2.4	20	48	DNA polymerase alpha suppressing protein kinase
TOR1	YJR066W	2.3	20	45	PI-3 kinase homolog, influences cell growth, DNA damage-induced recombination, G1-S checkpoint genes, potential targets: RPS6A+B, PHO85
PTK1	YKL198C	2.2	35	78	Serine/threonine protein kinase, acts in TOR signalling pathway
CTK3	YML112W	2.2	20	44	C-terminal domain (CTD) kinase gamma subunit, associates with Ctk1p and Ctk2p
SPO16	YHR153C	2.2	20	43	Sporulation protein
TOR2	YKL203C	2.1	29	61	PI-4 kinase, involved in cell growth, DNA damage induced recombination, G1-S progression, related to Tor1p
PCL10	YGL134W	2.1	30	62	Cyclin like protein interacting with Pho85p, putative TOR downstream target
PRP8	YHR165C	−5.2	104	20	U5 snRNA-associated splicing factor, component of the spliceosome
DDR48	YMR173W	−4.9	98	20	Stress protein induced by heat shock, DNA damage, or osmotic stress
?	YHL046C	−3.9	78	20	Similarity to members of the PAU1 family, repressed by TUP1
MCM3	YEL032W	−3.9	77	20	Acts at ARS elements to initiate replication; member of the MCM/P1 family, mutant shows hyper-rec phenotype
PKC1	YBL105C	−3.9	77	20	Protein kinase C, regulates map kinase cascade involved in regulating cell wall metabolism, mutant shows hyper-rec phenotype
HSF1	YGL073W	−3.7	73	20	Heat shock transcription factor, induces DDR48
DAK1	YML070W	−3.3	76	23	Dihydroxyacetone kinase, induced in high salt
VPS34	YLR240W	−3.3	65	20	PI-3 kinase, required for vacuolar protein sorting, activated by protein kinase Vps15p
PHO85	YPL031C	−3.0	59	20	Putative TOR downstream target, cyclin-dependent protein kinase that interacts with Pho80p-like cyclins to regulate phosphate pathway
TEC1	YBR083W	−3.0	59	20	Ty transcription activator, induces DDR48 and SPO12
SPT6	YGR116W	−2.7	54	20	Transcription elongation protein involved in chromatin structure that influences expression of many genes, mutant shows hyper-rec phenotype
BCK2	YER167W	−2.6	52	20	Involved in the SIT4 pathway for CLN1–3 activation and in suppression of lethality due to mutations in the protein kinase C pathway
GAT1	YFL021W	−2.6	51	20	Involved in TOR signalling, gata zinc finger transcription factor that plays a supplemental role to Gln3p
TAF90	YBR198C	−2.5	49	20	TFIID and SAGA subunit, required for activated transcription by RNA polymerase II
SIT4	YDL047w	−2.3	46	20	Serine/threonine phosphatase involved in cell cycle regulation; member of the PPP family of protein phosphatases and related to PP2a phosphatase
SIR4	YDR227W	−2.1	47	22	Silencing regulatory and DNA-repair coiled-coil protein
FUN30	YAL019W	−2.1	48	23	Similarity to helicases of the Snf2 (Swi2) protein family, recognizes transition between paired and unpaired DNA strands

ORFs showing a 2 or more fold change in expression are listed. Information on gene function and regulation was obtained from the sources indicated.

[a] Indicates ORF number.

[b] Ratio is respective to cells treated without toxin.

[c] Hybridization signal is given in arbitrary units of fluorescence.

[d] Description of gene function according to the Yeast Protein Database.

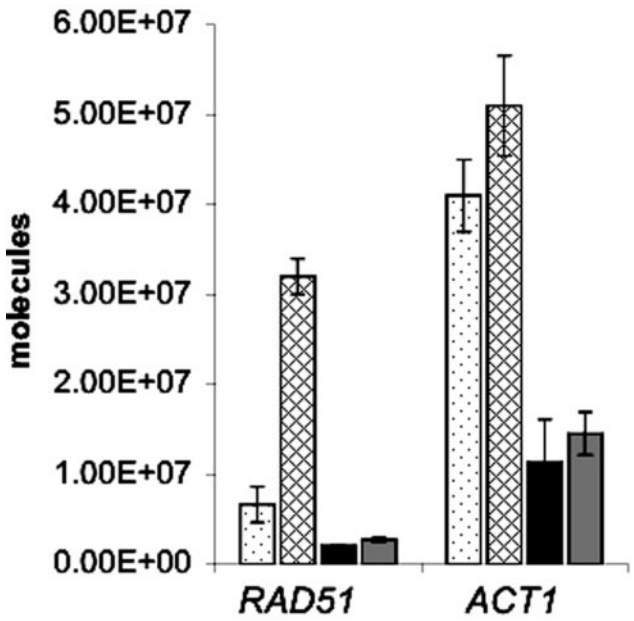

Figure 4. Quantitative RT-PCR of *RAD51* and *ACT1* RNA in *MEC1* (YB110 pCS316) and *mec1* (YB324 pCS316) strains after cells were exposed to 25 μM AFB_1. RNA was extracted from cells after a 4-h exposure. The vertical axis indicates the number of RNA molecules per 10 ng of total RNA. Three independent experiments were performed. Dot-filled bars represent untreated wild-type (*MEC1*) cells. Diagonal-filled bars represent AFB_1-treated wild-type cells. Black bars represent untreated *mec1*Δ cells, and gray bars represent AFB_1-treated *mec1*Δ cells. *mec1-21* (YB325 pCS316) cells gave similar results as the *mec1* null mutant.

Interestingly, numerous genes of the NER pathway were induced after AFB_1 exposure; these included *RAD1, RAD3, RAD16,* and *MET18*. *RAD1* functions in several *RAD51*-independent mitotic recombination events (Davies *et al.,* 1995; Saparbaev *et al.,* 1996; Paques and Haber, 1999; Aguilera *et al.,* 2000; Haber, 2000; Nicholson *et al.,* 2000) as well as in the spontaneous generation of homology-directed translocations (Fasullo *et al.,* 1998).

Several genes that are upregulated after AFB_1 exposure also function to decrease particular recombination events. For example, the Hpr5/Srs2 helicase is suggested to function as an antirecombinase preventing excessive and aberrant *RAD51*-mediated recombination events (Klein, 2000). In addition, some genes of the MMR pathway, including *MLH1, MLH3,* and *MSH6*, were induced, and Mlh1 and Mlh3 can both reduce recombination between repeated sequences containing mismatches (Nicholson *et al.,* 2000). Although the induction of these genes may seem contradictory to the notion that AFB_1 stimulates recombination, *HPR5/SRS2* is also upregulated in meiosis during which higher levels of heteroallelic and ectopic recombination occur. Mitotic, heteroallelic recombination is not decreased in mismatch repair mutants (Saparbaev *et al.,* 1996), and *msh2* mutants do not exhibit decreased mitotic recombination between *his3* fragments positioned on different chromosomes (unpublished data). Yeast Mlh1 interacts with Sgs1, a protein encoded by a human BLM homologue (Foury, 1997), and may be involved in some aspect of general recombination (Pedrazzi *et al.,* 2001). We also speculate that the induction of the mismatch repair proteins may contribute to the weak mutagenicity of AFB_1. Thus, the upregulation of *MSH6* and *HPR5* is consistent with the genotoxic properties of AFB_1.

Besides genes encoding DNA repair functions, genes involved in damage signaling, stress response, and cell cycle progression were also upregulated after AFB_1 exposure. Overexpression of *SPO12,* which was strongly induced (8.5-fold) after AFB_1 exposure, is thought to reduce cyclin-dependent kinase activity and trigger exit from mitosis (Shah *et al.,* 2001). The observation that 9 (*TOR1, TOR2, CTK1, MAD1, PTK1, PCL10, VPS34, PHO85, GAT1*) of 43 genes displaying at least twofold change in expression have func-

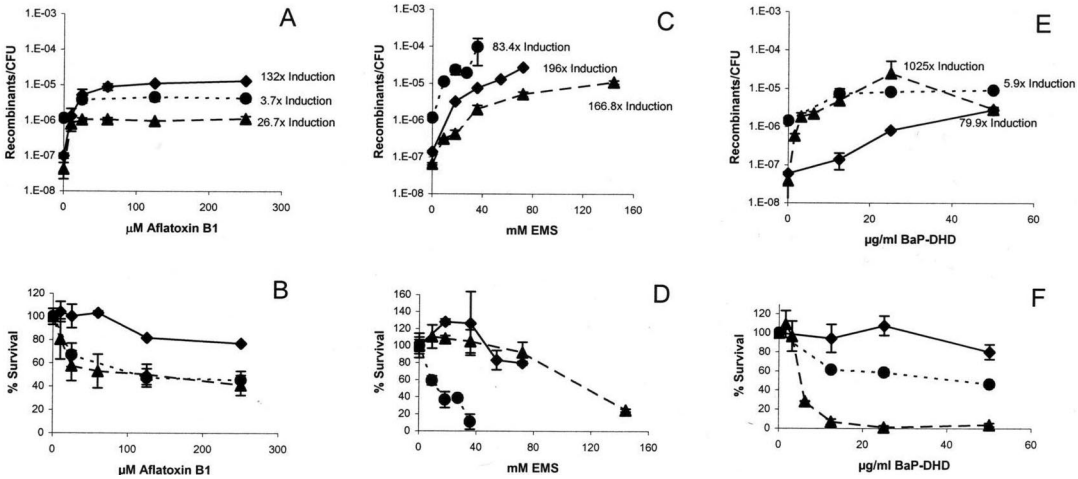

Figure 5. Induction of recombination and drug killing by AFB_1, EMS, and BaP-DHD in wild-type (♦), *rad1* (▲), and *rad51* (●) yeast strains. The *S. cerevisiae* strains YB150pCS512 (*rad1*), YB195pSB229 (*rad51*), and the repair proficient strain YB110pSB229 (wt) all express hCYP1A1 and hOR for metabolic activation of the toxic compounds. Recombination frequency was determined as His^+ recombinant/colony forming unit (CFU) and plotted against drug concentration. Survival percentage was calculated as the ratio of CFU after drug treatment to CFU before drug treatment multiplied by 100%. The ratio of the recombination frequencies obtained after drug exposure and before drug exposure, or fold induction, is indicated for selective drug concentrations. The means and standard deviations (bars) were calculated from two to five independent experiments. (A) and (B) Recombination frequencies and % survival after exposure to AFB_1. (C) and (D) Recombination frequencies and % survival after exposure to EMS. (E) and (F) Recombination frequencies and % survival after exposure to BaP-DHD.

Table 5. Translocation frequencies in wild-type, *mec1*, and *mec1* (pR51.3) strains

Genotype (strain)[a]	Survival (%)[b]	Translocation frequency ($\times 10^7$)[c]		Fold increase[e]
		Spontaneous[c]	AFB_1-associated[d]	
MEC1 (YB110 pCS316)	86	2.7 ± 1.2	69 ± 14	26
mec1–21 (YB325 pCS316)	80	24 ± 4	42 ± 14	1.8
sml1::*kanMX* (YB323 pCS316)	94	2.3 ± 1	10 ± 5	4.4
mec1::*TRP1 sml1*::*kanMX* (YB324 pCS316)	100	12 ± 9	15 ± 7	1.2
mec1–21 (YB325 pCS316, pR51.3)	55	49 ± 12	440 ± 250	9

[a] See text for complete genotype.

[b] CFU after 25 μm AFB_1 exposure/CFU before exposure × 100%.

[c] His^+ recombinants/total CFU.

[d] His^+ recombinants after AFB_1 exposure/total CFU after AFB_1 exposure.

[e] AFB_1-associated translocation frequency/spontaneous translocation frequency.

tions in TOR (target of rapamycin) signaling suggests a role of this pathway in response to AFB_1 toxicity. Genes involved in TOR signaling, including *VPS34* (phosphatidylinositol 3-kinase), are involved in regulatory mechanisms modulating protein synthesis and degradation and are important for promoting growth (Keith and Schreiber, 1995; Thomas and Hall, 1997; Dennis *et al.*, 1999). The significance of these genes may be further elucidated when specific cell cycle checkpoints are identified that are triggered by AFB_1 exposure.

The downregulation of some genes may also function to increase the recombinogenicity of AFB_1-induced DNA lesions. For example, the gene encoding protein kinase C (*PKC1*) is downregulated (3.9-fold decreased); null *pkc1* mutants are inviable and arrest during S phase, whereas other mutations in *PKC1* confer a hyper-recombinogenic phenotype (Huang and Symington, 1994). Mutations in two other AFB_1 downregulated signaling genes, *MCM3* and *SPT6*, also confer hyper-recombinogenic phenotypes (Aguilera *et al.*, 2000). These data provide further evidence that the downregulation as well as the upregulation of specific genes may contribute to the recombinogenic cellular response to AFB_1.

The mechanism by which the AFB_1-induced changes in gene expression increase recombination is unknown. However, these changes may aid in identifying genes that contribute to the genotoxicity of AFB_1, compared with other DNA-damaging agents. For example, AFB_1-associated recombination depends on the function of several AFB_1-inducible genes, such as *RAD1* and *RAD51*. We demonstrated that higher levels of *RAD51* message correlates with higher frequencies of AFB_1-associated translocations in checkpoint mutants deficient in *RAD51* induction. In mammalian cells overexpression of *RAD51* also increases the frequency of chromosomal rearrangements and translocations (Richardson *et al.*, 2004). Thus, an increase in *RAD51* levels in particular mammalian or yeast cells may increase recombination. Considering that mutations in upstream regulatory regions of other DNA damage-inducible genes, such as *RAD54*, do not confer a decrease in either radiation resistance or recombination (Cole and Mortimer, 1989), further experiments are necessary to understand whether *RAD51* induction per se is required for AFB_1-associated translocations.

We had previously observed that *rad51* diploid mutants exhibit 30- and 10-fold higher frequencies of translocations after x-ray and UV exposure, respectively (Fasullo *et al.*, 2001), whereas, *rad1* mutants exhibit decreased frequencies of x-ray–associated translocations (Fasullo *et al.*, 1998), compared with wild type. Higher frequencies of x-ray–associated translocations were detected in *rad51* mutants even when survival was low (Fasullo *et al.*, 2001). Thus, it is unlikely that AFB_1-induced lethality caused the recombination defect. Most His^+ recombinants generated in the *rad51* mutant contained nonreciprocal translocations; whereas the majority of translocations identified after AFB_1 and UV exposure in wild-type strains are reciprocal translocations. Nonreciprocal translocations may occur by break-induced replication (BIR) when a DNA polymerase replicates past a single-strand nick or when chromosomal fragments are inherited in subsequent divisions (Fasullo *et al.*, 1998). Considering that we are unable to detect chromosomal fragments after AFB_1 exposure, we speculate that AFB_1 lesions do not trigger replication fork collapse.

RAD1 and *RAD51* play a different function in EMS or BaP-DHD–associated recombination (Figure 6). Although DNA damage generated by alkylating agents, such as EMS, is mainly repaired by BER (Friedberg *et al.*, 1995), DNA damage that results from agents that form bulky adducts, such as BaP-DHD, is mainly repaired by NER (Hess *et al.*, 1997). *rad1* mutants are more sensitive to AFB_1 than to EMS and are extremely sensitive to BaP-DHD; this suggests that NER is not the main pathway or is redundant in the repair of AFB_1 lesions. We speculate that AFB_1-induced lesions may require *RAD1* to either initiate or process a recombination intermediate; *RAD1*-dependent recombination pathways have been extensively demonstrated by different groups (for review see Aguilera *et al.*, 2000; Haber, 2000; Sung *et al.*, 2000) and may participate in crossing-over (Symington *et al.*, 2000). Interestingly, BaP-DHD is more recombinogenic in *rad1* mutants than in wild-type strains, suggesting that more recombination events occur when the bulky adduct is not excised.

Similarly, *rad51* mutants are more sensitive to EMS than to AFB_1, indicating that *RAD51* is involved in repair of AFB_1 lesions, but more important in the repair of EMS lesions. The stimulation of recombination by particular alkylating agents, such as EMS, is dependent on cell division, suggesting that EMS-associated recombination occurs after the DNA polymerase encounters the unrepaired lesion (Galli and Schiestl, 1999; Aguilera *et al.*, 2000). The hypersensitivity

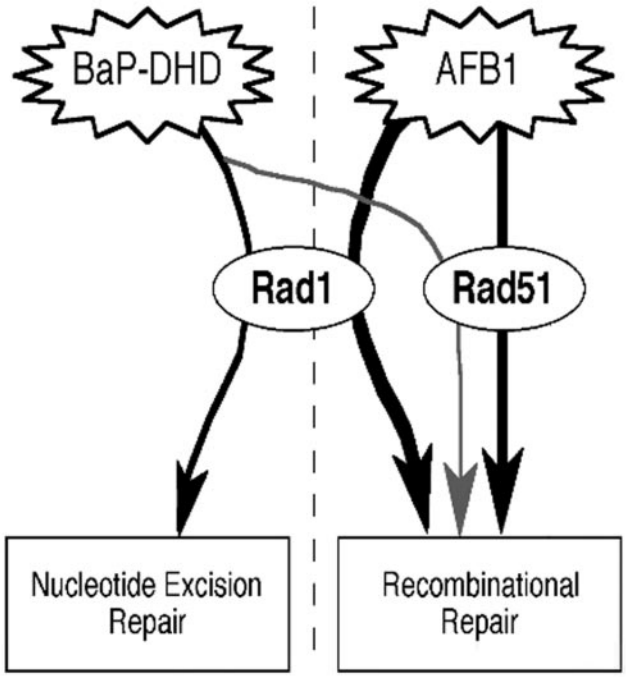

Figure 6. Role of *RAD1* and *RAD51* in the different repair pathways for DNA damage caused by AFB_1, EMS, and BaP-DHD. Models are derived from the results obtained with *rad1* and *rad51* mutants. The repair of AFB_1-induced DNA damage involves both *RAD1* and *RAD51*, and *RAD1* is required for recombinational repair of AFB_1-induced DNA damage. *RAD1* is required for the excision of BaP-DHD–induced DNA adducts, and *rad1* mutants exhibit higher frequencies of BaP-DHD–associated translocations, possibly due to the persistence of BaP-DHD–induced DNA adducts.

of the *rad51* strain to EMS likely results from the *rad51* defect in double-strand break repair; we speculate that double-strand breaks could be generated during BER if a DNA polymerase transverses a single-strand nick or gap and could stimulate a BIR mechanism. Additional experiments would be necessary to demonstrate that BER is a mechanism for generating more EMS-induced translocations in *rad51* mutants.

DNA damage and the subsequent repair are thought to account largely for the carcinogenicity of AFB_1. Recombinogenicity of a genotoxin could be pivotal in carcinogenesis as demonstrated by negative results in several mutagenesis tests (Schiestl, 1989; Galli and Schiestl, 1995, 1998). Results shown here help elucidate mechanisms by which changes in gene expression contribute to the genotoxicity of a compound. It will be interesting to investigate whether AFB_1 also changes the gene expression of orthologous genes in mammalian cells.

ACKNOWLEDGMENTS

We thank B. Weibel and H. Chen for excellent technical support. This work was supported by Grant 0-200-96 from the Swiss Federal Institute of Technology Zurich to C.S. and by Grant CA70105 to M.T.F. We thank Cinzia Cera for carefully reading this manuscript and Fumin Tong for advice concerning QPCR.

REFERENCES

Aguilera, A., Chavez, S., and Malagon, F. (2000). Mitotic recombination in yeast: elements controlling its incidence. Yeast, *16*, 731–754.

Bailey, G.S. (1994). Role of aflatoxin-DNA adducts in the cancer process. In: The Toxicology of Aflatoxins: Human Health, Veterinary, and Agricultural Significance, ed. D.L. Eaton and J.D. Groopmann, San Diego: Academic Press, 137–148.

Buss, P., Caviezel, M., and Lutz, W.K. (1990). Linear dose-response relationship for DNA adducts in rat liver from chronic exposure to aflatoxin B1. Carcinogenesis *11*, 2133–2135.

Cole, G.M., and Mortimer, R.K. (1989). Failure to induce a DNA repair gene, RAD54, in Saccharomyces cerevisiae does not affect DNA repair or recombination phenotypes. Mol. Cell. Biol. *9*, 3314–3322.

Croy, R.G., Essigmann, J.M., Reinhold, V.N., and Wogan, G.N. (1978). Identification of the principal aflatoxin B1-DNA adduct formed in vivo in rat liver. Proc. Natl. Acad. Sci. USA *75*, 1745–1749.

Croy, R.G., and Wogan, G.N. (1981). Quantitative comparison of covalent aflatoxin-DNA adducts formed in rat and mouse livers and kidneys. J. Natl. Cancer Inst. *66*, 761–768.

Davies, A.A., Friedberg, E.C., Tomkinson, A.E., Wood, R.D., and West, S.C. (1995). Role of the Rad1 and Rad10 proteins in nucleotide excision repair and recombination. J. Biol. Chem. *270*, 24638–24641.

Dennis, P.B., Fumagalli, S., and Thomas, G. (1999). Target of rapamycin (TOR): balancing the opposing forces of protein synthesis and degradation. Curr. Opin. Genet. Dev. *9*, 49–54.

Dong, Z., and Fasullo, M. (2003). Multiple recombination pathways for sister chromatid exchange in *Saccharomyces cerevisiae*: role of *RAD1* and the *RAD52* epistasis group genes. Nucleic Acids Res. *10*, 2576–2585.

Eaton, D.L., and Gallagher, E.P. (1994). Mechanisms of aflatoxin carcinogenesis. Annu. Rev. Pharmacol. Toxicol. *34*, 135–172.

Elledge, S.J., and Davis, R.W. (1990). Two genes differentially regulated in the cell cycle and by DNA damaging agents encode alternative regulatory subunits of ribonucleotide reductase. Genes Dev. *4*, 740–751.

Essigmann, J.M., Croy, R.G., Nadzan, A.M., Busby, W.F.J., Reinhold, V.N., Buchi, G., and Wogan, G.N. (1977). Structural identification of the major DNA adduct formed by aflatoxin B1 in vitro. Proc. Natl. Acad. Sci. USA *74*, 1870–1874.

Etienne, W., Meyer, M.H., Peppers, J., and Meyer, R.A. (2004). Comparison of mRNA gene expression by RT-PCR and DNA microarray. Biotechniques 36, 618–626.

Eugster, H.P., Bärtsch, S., Würgler, F.E., and Sengstag, C. (1992). Functional co-expression of human oxidoreductase and cytochrome P450 1A1 in *Saccharomyces cerevisiae* results in increased EROD activity. Biochem. Biophys. Res. Commun. *185*, 641–647.

Fasullo, M., and Dave, P. (1994). Mating type regulates the radiation-associated stimulation of reciprocal translocation events in *Saccharomyces cerevisiae.* Mol. Gen. Genet. *243*, 63–70.

Fasullo, M.T., and Davis, R.W. (1987). Recombination substrates designed to study recombination between unique and repetitive sequences in vivo. Proc. Natl. Acad. Sci. USA *84*, 6215–6219.

Fasullo, M.T., Bennett, T., AhChing, P., and Koudelik, J. (1998). The *Saccharomyces cerevisiae RAD9* checkpoint reduces the DNA damage-associated stimulation of directed reciprocal translocations. Mol. Cell. Biol. *18*, 1190–2000.

Fasullo, M.T., Giallanza, P., Bennett, T., Cera, C., and Dong, Z. (2001). Saccharomyces cerevisiae rad51 mutants are defective in DNA damage-stimulated sister chromatid exchange but exhibit increase rates of homology-directed translocations. Genetics *158*, 959–972.

Foury, F. (1997). Human genetic diseases: a cross-talk between man and yeast. Gene *195*, 1–10.

Friedberg, E.C., Walker, G.C., and Siede, W. (1995). DNA Repair and Mutagenesis, Washington, DC: ASM Press.

Galli, A., and Schiestl, R.H. (1995). Salmonella test positive and negative carcinogens show different effects on intrachromosomal recombination in G2 cell cycle arrested yeast cells. Carcinogenesis *16*, 659–663.

Galli, A., and Schiestl, R.H. (1998). Effect of Salmonella assay negative and positive carcinogens on intrachromosomal recombination in S-phase arrested yeast cells. Mutat. Res. *419*, 53–68.

Galli, A., and Schiestl, R.H. (1999). Cell division transforms mutagenic lesions into deletion-recombinagenic lesions in yeast cells. Mutat. Res. *429*, 13–26.

Gasch, A., Spellman, P., Kao, C., Carmel-Harel, O., Eisen, M., Storz, G., Botstein, D., and Brown, P.O. (2000). Genomic expression programs in the response of yeast cells to environmental changes. Mol. Biol. Cell *11*, 4241–4257.

Gasch, A., Huang, M., Metzner, S., Botstein, D., Elledge, S., and Brown, P. (2001). Genomic expression responses to DNA-damaging agents and the

regulatory role of the yeast ATR homolog Mec1p. Mol. Biol. Cell *12*, 2987–3003.

Goffeau, A. *et al.* (1996). Life with 6000 genes. Science *274*, 563–547.

Goldstein, A.L., and McCusker, J.H. (1999). Three new dominant drug resistance cassettes for gene disruption in *Saccharomyces cerevisiae*. Yeast *15*, 1541–1553.

Haber, J.E. (2000). Recombination: a frank view of exchanges and vice versa. Curr. Opin. Cell. Biol. *12*, 286–292.

Hess, M.T., Gunz, D., Luneva, N., Geacintov, N.E., and Naegeli, H. (1997). Base pair conformation-dependent excision of benzo[a]pyrene diol epoxide-guanine adducts by human nucleotide excision repair enzymes. Mol. Cell. Biol. *17*, 7069–7076.

Hsu, I.C., Metcalf, R.A., Sun, T., Welsh, J.A., Wang, N.J., and Harris, C.C. (1991). Mutational hotspot in the p53 gene in human hepatocellular carcinomas. Nature *350*, 427–428.

Huang, K., and Symington, L. (1994). Mutation of the gene encoding protein kinase C1 stimulates mitotic recombination in *Saccharomyces cerevisiae.* Mol. Cell. Biol. *14*, 6039–6045.

Jelinsky, S.A., and Samson, L.D. (1999). Global response of *Saccharomyces cerevisiae* to an alkylating agent. Proc. Natl. Acad. Sci. USA *96*, 1486–1491.

Keith, C.T., and Schreiber, S.L. (1995). PIK-related kinases: DNA repair, recombination, and cell cycle checkpoints. Science *270*, 50–51.

Keller-Seitz, M. (2001). PhD thesis no. 14321. Swiss Federal Institute of Technology (ETH).

Klebe, R.J., Harriss, J.V., Sharp, Z.D., and Douglas, M.G. (1983). A general method for polyethylene-glycol-induced genetic transformation of bacteria and yeast. Gene *25*, 333–341.

Klein, H.L. (2000). A radical solution to death. Nat. Genet. *25*, 132–134.

Leadon, S.A., Tyrrell, R.M., and Cerutti, P.A. (1981). Excision repair of aflatoxin B1-DNA adducts in human fibroblasts. Cancer Res. *41*, 5125–5129.

Lin, J.-K., Miller, J.A., and Miller, E.C. (1977). 2,3-Dihydro-2-(guan-7-yl)-3-hydroxy-aflatoxin B1, a major acid hydrolysis product of aflatoxin B1-DNA or -ribosomal RNA adducts formed in hepatic microsome-mediated reactions in rat liver in vivo. Cancer Res. *37*, 4430–4438.

Martin, C.N., and Garner, R.C. (1977). Aflatoxin B1-oxide generated by chemical or enzymatic oxidation of aflatoxin B1 causes guanine substitution in nucleic acids. Nature *267*, 863–865.

Mercier, G., Denis, Y., Marc, P., Picard, L., and Dutriex, M. (2001). Transcriptional induction of repair genes during slowing of replication in irradiated *Saccharomyces cerevisiae.* Mutat. Res. *487*, 157–172.

Mewes, H.W., Albermann, K., Heumann, K., Liebl, S., and Pfeiffer, F. (1997). MIPS: a database for protein sequences, homology data and yeast genome information. Nucleic Acids Res. *25*, 28–30.

Nicholson, A., Hendrix, M., Jinks-Robertson, S., and Crouse, G.F. (2000). Regulation of mitotic homeologous recombination in yeast. Functions of mismatch repair and nucleotide excision repair genes. Genetics *154*, 133–146.

Otteneder, M., and Lutz, W.K. (1999). Correlation of DNA adduct levels with tumor incidence: carcinogenic potency of DNA adducts. Mutat. Res. *424*, 237–247.

Paques, F., and Haber, J.E. (1999). Multiple pathways of recombination induced by double-strand breaks in *Saccharomyces cerevisiae*. Microbiol. Mol. Biol. Res. *63*, 349–404.

Payne, W.E., and Garrels, J.I. (1997). Yeast Protein database (YPD): a database for the complete proteome of *Saccharomyces cerevisiae.* Nucleic Acids Res. *25*, 57–62.

Pedrazzi, G., et al. (2001). Direct association of Bloom's syndrome gene product with the human mismatch repair protein. MLH1. Nucleic Acids Res. *29*, 4378–4386.

Posas, F., Chambers, J.R., Heyman, J.A., Hoeffler, J.P., de Nadal, E., and Arino, J. (2000). The transcriptional response of yeast to saline stress. J. Biol. Chem. *275*, 17249–17255.

Richardson, C., Stark, J.M., Ommundsen, M., and Jasin, M. (2004). Rad51 overexpression promotes alternative double-strand break repair pathways and genome instability. Oncogene *23*, 546–553.

Sanchez, Y., Desany, B.A., Jones, W.J., Liu, Q., Wang, B., and Elledge, S.J. (1996). Regulation of *RAD53* by the ATM-like kinases *MEC1* and *TEL1* in yeast cell cycle checkpoint pathways. Science *27*, 357–360.

Saparbaev, M., Prakash, L., and Prakash, S. (1996). Requirement of mismatch repair genes *MSH2* and *MSH3* in the *RAD1-RAD10* pathway of mitotic recombination in *Saccharomyces cerevisiae.* Genetics *142*, 727–736.

Schiestl, R.H. (1989). Nonmutagenic carcinogens induce intrachromosomal recombination in yeast. Nature *337*, 285–288.

Sengstag, C., Weibel, B., and Fasullo, M. (1996). Genotoxicity of aflatoxin B_1: evidence for a recombination-mediated mechanism in *Saccharomyces cerevisiae.* Cancer Res. *56*, 5457–5465.

Shah, R. Jensen, S., Frenz., L. M., Johnson, A.L., and Johnston, L.H. (2001). The Spo12 protein of *Saccharomyces cerevisiae*: regulator of mitotic exit whose cell cycle-dependent degradation is mediated by the anaphase-promoting complex. Genetics *159*, 965–980.

Shen, H.M., and Ong, C.N. (1996). Mutations of the p53 tumor suppressor gene and ras oncogenes in aflatoxin hepatocarcinogenesis. Mutat. Res. Rev. Genet. Toxicol. *366*, 23–44.

Shirra, M.K., Patton-Vogt, J., Ulrich, A., Liuta-Tehlivets, O., Kohlwein, S.D., Henry, S.A., and Arndt, K.M. (2001). Inhibition of acetyl coenzyme A carboxylase activity restores expression of the *INO1* gene in a *snf1* mutant strain of *Saccharomyces cerevisiae.* Mol. Cell. Biol. *21*, 5710–5722.

Smela, M.E., Currier, S.S., Bailey, E.A., and Essigmann, J.M. (2001). The chemistry and biology of aflatoxin B *1*, from mutational spectrometry to carcinogenesis. Carcinogenesis *22*, 535–545.

Stettler, P., and Sengstag, C. (2001). Liver carcinogen aflatoxin B1 as an inducer of mitotic recombination in a human cell line. Mol. Carcinog. *31*, 125–138.

Sung, P. (1994). Catalysis of ATP-dependent homologous DNA pairing and strand exchange by yeast *RAD51* protein. Science, *265*, 1241–1243.

Sung, P., and Robberson, D.L. (1995). DNA strand exchange mediated by a RAD51-ssDNA nucleoprotein filament with polarity opposite to that of RecA. Cell *82*, 453–461.

Sung, P., and Stratton, S.A. (1996). Yeast Rad51 recombinase mediates polar DNA strand exchange in the absence of ATP hydrolysis. J. Biol. Chem. *271*, 27983–27986.

Sung, P., Trujillo, K.M,. and Van Komen, S. (2000). Recombination factors of *Saccharomyces cerevisiae*. Mutat. Res. *451*, 257–275.

Symington, L., Kang, L., and Moreau, S. (2000). Alteration of gene conversion tract length and associated crossing over during plasmid gap repair in nuclease-deficient strains of *Saccharomyces cerevisiae*. Nucleic Acids Res. *28*, 4649–4656.

Thomas, G., and Hall, M.N. (1997). TOR signaling and control of cell growth. Curr. Opin. Cell Biol. *9*, 782–787.

Wodicka, L., Dong, H., Mittmann, M., Ho, M.H., and Lockhart, D.J. (1997). Genome-wide expression monitoring in *Saccharomyces cerevisiae*. Nat. Biotechnol. *15*, 1359–1367.

Wogan, G.N. (1999). Aflatoxin as a human carcinogen. Hepatology *30*, 573–575.

Zhao, X., Muller, E.G., and Rothstein, R. (1998). A suppressor of two essential checkpoint genes identifies a novel protein that negatively affects dNTP pools. Mol. Cell *2*, 329–340.

Zhao, X., Georgieva, B., Chabes, A., Domkin, V., Ippel, J.H., Schleucher, J., Wijmenga, S., Thelander, L. (2000). Mutational and structural analyses of the ribonucleotide reductase inhibitor Sml1 define its Rnr1 interaction domain whose inactivation allows suppression of *mec1* and *rad53* lethality. Mol. Cell. Biol. *20*, 9076–9083.